Portable Sensors for Breath Analysis

by

Amlendu Prabhakar

A Dissertation Presented in Partial Fulfillment
of the Requirements for the Degree
Doctor of Philosophy

Approved August 2013 by the
Graduate Supervisory Committee:

Nongjian Tao, Chair
Erica Forzani
Stuart Lindsay

ARIZONA STATE UNIVERSITY

December 2013

ABSTRACT

Human breath is a concoction of thousands of compounds having in it a breath-print of physiological processes in the body. Though breath provides a non-invasive and easy to handle biological fluid, its analysis for clinical diagnosis is not very common. Partly the reason for this absence is unavailability of cost effective and convenient tools for such analysis. Scientific literature is full of novel sensor ideas but it is challenging to develop a working device, which are few. These challenges include trace level detection, presence of hundreds of interfering compounds, excessive humidity, different sampling regulations and personal variability.

To meet these challenges as well as deliver a low cost solution, optical sensors based on specific colorimetric chemical reactions on mesoporous membranes have been developed. Sensor hardware utilizing cost effective and ubiquitously available light source (LED) and detector (webcam/photo diodes) has been developed and optimized for sensitive detection. Sample conditioning mouthpiece suitable for portable sensors is developed and integrated. The sensors are capable of communication with mobile phones realizing the idea of m-health for easy personal health monitoring in free living conditions.

Nitric oxide and Acetone are chosen as analytes of interest. Nitric oxide levels in the breath correlate with lung inflammation which makes it useful for asthma management. Acetone levels increase during ketosis resulting from fat

metabolism in the body. Monitoring breath acetone thus provides useful information to people with type1 diabetes, epileptic children on ketogenic diets and people following fitness plans for weight loss.

DEDICATION

I would like to dedicate this thesis to my teacher and divine mother Shri Mataji Nirmala Devi and also to my parents. Their guidance and love are constant sources of strength in my life.

ACKNOWLEDGEMENTS

The years I have spent working on this thesis have enriched my life in many ways. This could be accomplished with help of many people's support, guidance, and encouragement. My advisor, Prof. NJ Tao has always been a big support. He has shaped me into a researcher by teaching my how to ask pertinent questions and then seek the right answers. I am grateful for his guidance. Dr. Rodrigo Iglesisas with whom I worked in the course of my first project has been a great mentor. I thank him for teaching me how to setup experiments, how to reason, and how to work with colleagues. His presence in the beginning of my graduate studies was a blessing. My committee member Dr. Erica Forzani with whom I have worked very closely during my last project has taught me the value of hard work by example and helped me become an independent researcher. I am thankful for her kindness and support. Dr. Francis Tsow has always been a mentor, friend, and a helping hand in the lab. His presence around has saved me numerous sleepless nights in the lab. I sincerely thank him for his help. Like my mentors, other lab members and fellow students have also played an equally important role during my graduate studies at Arizona State University. I have spent countless number of hours in discussions, experimental setups, debugging, joking, and dreaming about future with Rui, Lihua, Ashley, Xiaojun, Xhaonan, Cheng, Di, and Devon. They all deserve my profound gratitude. I am also grateful to all my friends at sahaja yoga mediation center in Phoenix. They have been my family all these years. I have never felt alone or stressed during my graduate

studies because of them. Lastly and most importantly I am indebted to my parents and sister for having the courage to part with me for five long years. They have been extremely supportive in all my endeavors and I am lucky to have them as my family.

TABLE OF CONTENTS

Page

CHAPTER Page

CHAPTER Page

LIST OF TABLES

Table Page

LIST OF FIGURES

Figure Page

Figure Page

Figure Page

Figure Page

Figure Page

INTRODUCTION

Clinical diagnosis is based on inferences that are drawn on information collected about our body in a diseased condition or otherwise. With advancements in molecular diagnostics we are no more limited to just physical examination to tell us the story. Biological fluids are very routinely analyzed in a clinical laboratory to aid in diagnosis and narrow down to specific conclusions. The main focus of the biochemical and biomolecular diagnostic methods which have developed very rapidly in past few decades has been on blood and urine analysis. Considering that medical diagnosis is driven by information, it becomes important to consider all available sources of information.

Breath is another biological fluid which has not been exploited to its full potential for clinical diagnosis. A question that may be asked at this point is that given all the advances made in blood and urine analysis, do we gain any new information out of breath analysis? Blood or urine tests are usually concerned with large molecules which are non-volatile in nature such as proteins and other macromolecules. Low molecular weight volatile compounds are usually lost in sampling. However, it is now evident that many of these volatile compounds are found in exhaled breath even though they are in trace concentrations of parts per million (ppm) or parts per billion (ppb) by volume [3]. Many of these compounds, when quantitatively measured, can give us information for appropriate diagnosis [4].

Apart from having information that is not available by routine blood and urine analysis, breath analysis is also attractive because it is a non-invasive procedure [5]. It is more agreeable to patients over blood sampling which is invasive and considered painful and also over urine sampling due to convenience of sample availability which avoids embarrassment to the patient [6]. Breath samples have successfully been collected from a range of subjects including neonates [7], conscious two year old children [8], critically ill patients [9], and patients with Alzheimer's and Parkinson's disease [10].

With all the potentials of clinical diagnostics and ease of sample access, exhaled breath analysis has attracted attentions of scientists and engineers. Even though a lot of work has been done in recent past, using breath for diagnosis is not a new concept. Historically, ancient Greek and Chinese medical texts have associated unique breath smells with physiological disorders or diseases. Likewise, breath smells of patients with uncontrolled diabetes are often described as rotten apple like due to high acetone levels in their breath, failing kidneys can lead to urine-like smell in the breath due to ammonia buildup, patients with lung abscesses may have sewer like smell in their breath due to proliferation of anaerobic bacteria, and a fishy reek smell may be the result of a liver disease [11-13]. The limitation of relying on breath smell for diagnosis is that diseases can only be diagnosed at a very advanced stage when systemic metabolism has been totally compromised.

Today, a lot more is known both qualitatively and quantitatively about the exhaled breath. With advancement in analytical techniques, several studies have contributed to our understanding of breath as a complex mixture of gases. Starting from

Lavoisier who analyzed exhaled breath and reported the first quantitative analysis of carbon dioxide in 1784 to various modern pioneering works from Pauling [14], Larson [15], Chen [16], Riely [17], Phillips [18] and others have helped to identify more than 3,500 different components in exhaled breath. The composition of exhaled breath is now identified as a mixture of inorganic gases (e.g. NO, CO_2 and CO), volatile organic compounds (VOCs) (e.g. isoprene, ethane, pentane, and acetone), and other typically nonvolatile substances (e.g. isoprostanes, peroxynitrite, cytokines and nitrogen).

Since these components are of endogenous and also exogenous origin, they carry signatures of various physiological processes that take place in the body [3, 19] and also can reflect one's environmental exposure. This signature has been referred to as breath print in the literature [10, 20]. Many studies have been done to understand the origin of these gases in exhaled breath or to correlate their quantitative levels to certain physiological states. The understanding of this breath print in individuals or populations aims to establish either the presence or changes in concentrations of some of the exhaled components as markers for diagnosis and/or monitoring of our health or monitoring the therapy administered under diseased conditions.

United States Federal Drug Administration (FDA) has approved breath testing for monitoring blood alcohol using breath ethanol, asthma using exhaled nitric oxide, neonate jaundice using exhaled carbon monoxide, testing for Helicobacter pylori infection using exhaled carbon dioxide, carbohydrate metabolism using hydrogen and organ transplant rejection using exhaled branched hydrocarbons. This list will hopefully grow rapidly as more and more pilot studies are being done to establish changes in some

other breath components as indicative of diseases. For example, acetone levels are seen elevated in diabetes [21], higher ammonia levels indicate kidney and liver dysfunction [22, 23], and saturated hydrocarbon levels can be used to monitor the degree of oxidative stress [24, 25].

To gain further knowledge about how breath reflects our health is an important task at hand but equally important is to develop tools which will allow us to use the knowledge already available to the field of breath research in monitoring health, fitness and therapies in a facile and economical manner. Several tools available for breath analysis include gas chromatography coupled with mass spectrometry (GC-MS) or flame ionization detection (GC-FID), Selected Ion Flow Tube mass spectrometry (SIFT-MS), Chemiluminescence detection, Laser spectroscopy, and electrochemical sensors. Many of these tools though are very accurate, do not go beyond a laboratory or clinical setting because they are either very expensive, bulky, or need expertise for operation.

To utilize breath as a tool for monitoring of health and fitness, people should be empowered with sensor devices that can come out of a standard laboratory or clinical setting and be used on a regular basis. For this reason, ideas from mobile health technologies popularly known as m-health have inspired development of the sensors presented in this thesis. The term m-health, coined by Prof. Robert Istepania, is referred to as “emerging mobile communications and network technologies for healthcare systems” in his book M-Health: Emerging Mobile Health Systems [26] and it was defined as “the delivery of healthcare services via mobile communication devices” at the 2010 mHealth Summit of the Foundation for the National Institutes of Health [27].

Modern health care faces several challenges in terms of rising costs, increasing demand, lack of trained health care professionals and facilities, poor reach in remote areas and limited financial resources [28]. Under these constrains it becomes important to look up to development in other technological areas for solutions. Mobiles phones have become ubiquitous not only in developed countries but in many developing countries too [29]. Their penetration into remote areas present a unique opportunity for delivering health care to inaccessible places utilizing capabilities of information technology [30]. Internet enabled smart phones take it to the next level where phones are not only limited to delivering information but can be used to communicate with external devices, process large chunks of data, present processed results to the user or a health care professional, create cloud accessible logs, and be remotely updated. Thus, m-health promises to provide solutions for ubiquitous monitoring of health in rural or urban free living conditions which would help in better health management of the users, regular monitoring also would help reduce emergency health situations by providing timely alarm to impending health issues. Many efforts to exploit the potentials of m-health have been made. Many physical sensors have been integrated with mobile phones. These can read EEG and ECG signal using electrodes [31-34], movement using accelerometers [35], blood oxygen levels and heart rates using optical detection [36], calorie intake using phone's inbuilt cameras [37, 38], and offer health related motivational and educational games [39, 40]. Chemical sensors are not as popular in m-health domain except some electrochemical sensors for blood glucose measurements [41, 42]. This is mainly because miniaturization and then integration of chemical sensors with mobile technologies is

challenging. This becomes even more difficult with breath sensors. To meet these requirements there are several characteristics that such a sensor should have. It should have a sensitive detection to monitor trace gases because several compounds of interest are only available in ppb or ppm levels by volume in the breath. Breath being a complex mixture of thousands of trace gases also requires the sensor to be selective towards the component to be analyzed. If confounded, either by other trace gases or components in high concentrations like oxygen, carbon dioxide, and water vapors, the sensor is rendered useless. There should be facility for consistent breath sample delivery and conditioning of the sample. Many times, the breath sensors cannot be made immune to all the interfering components. Even if the detection is specific, high amount of water vapors condensed in the sampling line or sensor surface can lead to either confounding, blockage, or noise in the signal. There are also situations in which the components as such cannot be detected but are detectable after certain preconditioning. For example, oxidation, reduction, or conversion to other forms by a suitable chemical reaction. Appropriate measures should be included in the device to precondition the sample before analysis in order to avoid these issues encountered during online sampling. The sensor device, if targeted towards use by people in general should also be small. The question one may ask is, how small is small? Of course, it depends on the usage. Considering the application to be regular monitoring of health in a free living condition not confined to hospitals, a wearable size would be most appropriate. Also the cost of such a sensor device would play a role in deciding its reach to people. Though certain critically ill patients who would need regular monitoring on an urgent basis may justify high spending on such a device, in many other

cases where monitoring is needed but is not urgent, high cost may be a deterrent. An expensive device may not at all be affordable to many people who may be in urgent need of monitoring. Certainly, available tools which cost from few thousand dollars in case of electrochemical sensors to above hundred thousand dollars in case of SIFT-MS are not easily affordable. Also cost per test and the maintenance required are important factors. The lower the investment and the running cost the more is the acceptability of the system to general people for regular use.

This thesis describes development of breath sensors for monitoring exhaled nitric oxide and acetone using optical detection. Exhaled nitric oxide is an FDA approved marker for monitoring asthma and acetone has applications in monitoring fat oxidation and the resulting ketone build up in the blood. The detection based on colorimetric changes is effectively realized using a low cost sensing platform. The detection chemistry has been supported on inexpensive substrates for lower cost per test. Appropriate measures are described to ensure proper online sampling. Real tests were made to show the applicability of the developed sensors as tools for use by people in general.

2

BACKGROUND

2.1 Breath as a clinical sample

With emergence of advanced analytical techniques exhaled breath is no more just a mixture of nitrogen, oxygen, carbon dioxide, and water vapors. Pauling and his coworkers, using gas liquid partition chromatography presented in 1971 that breath has a complex composition. Even though without identification, he showed existence of 250 volatile organic compounds in exhaled breath of subjects on a defined diet [14]. Since unique smells from breath of patients has been used for diagnosis for a long time, this demonstration from Pauling motivated many studies to understand breath compositions with a view that components in exhaled breath may have clinically important data which was unavailable from routine clinical tests. In the next decade about 200 compounds were identified in exhaled breath [43-46]. Several of these compounds have trace concentrations in sub ppb and sub ppm levels by volume (Table 2.1). With new and improved analytical methods resulting in higher sensitivity and better sampling methods, discovery of new components in breath accelerated and now we have a list of more than 1000 compounds in human breath. These compounds in the breath may result from endogenous metabolic processes or may be absorbed as a result of exposure from contaminated environment. For this reason exhaled breath has been explored both for monitoring metabolic or pathologic process in the body and environmental exposure.

Table 2.1: Dynamic range of concentration of some compounds present in exhaled breath [47]

Concentration (v/v)	Molecule
Percentage (%)	Oxygen, water, carbon dioxide
parts per million (ppm)	Acetone, carbon monoxide, methane, hydrogen
parts per billion (ppb)	Formaldehyde, acetaldehyde, isoprene, 1-pentane, ethane, other hydrocarbons, nitric oxide, carbon disulfide, methanol, carbonyl sulfide, methanethiol, ammonia, methylamine, dimethyl sulfide

The idea of monitoring physiological processes via breath analysis is based on the assumption that there is a gaseous equilibrium between alveolar air and pulmonary blood. This means that the exhaled breath gas concentrations are correlated with their respective blood concentrations. This direct proportionality between the alveolar concentration C_A of a VOC and its concentration in the venous blood C_B is given by Farhi equation [48, 49].

$$C_A = \frac{C_B}{\lambda_{b:air} + \frac{\dot{V}_A}{Q_C}} \qquad (2.1)$$

Here, $\lambda_{b:air}$ is the substance specific blood gas partition coefficient which describes the diffusion equilibrium in the respiratory microvasculator, $\dot{V}_A$ is the alveolar ventilation which governs the transport of the compound through the respiratory track,

and $\dot{Q}_C$ is the cardiac output which controls the rate at which the compound delivered to the lungs. Considering lung to be a homogenous alveolar unit, end capillary blood concentration $C_{C'}$, blood inflow/outflow $\dot{Q}_C$ and gas inflow/outflow $\dot{V}_A$, mass conservation give us the following relationship

$$V_A \frac{dC_A}{dt} = \dot{V}_A(C_I - C_A) + \dot{Q}_C(C_B - C_{C'}) \qquad (2.2)$$

Here V_A is the volume of the pulmonary space for the gas under consideration, and C_I is its concentration in the inspired air. Considering C_I to be negligible and assuming steady state condition i.e. $C_{C'} = \lambda_{b:air} C_A$ implying no accumulation in the lungs and diffusion equilibrium to hold, the relationship becomes

$$\dot{V}_A C_A = \dot{Q}_C(C_B - \lambda_{b:air} C_A) \quad (2.3)$$

which leads to the Farhi equation

$$C_A = \frac{C_B}{\lambda_{b:air} + \frac{\dot{V}_A}{\dot{Q}_C}} \qquad (2.4)$$

This equation represents a simplified equilibrium description of the gaseous mass balance in the lungs. Several experimental and modeling approaches have been presented to extend it to chemically bound gases and non-equilibrium processes for it to be applicable to a wide range of VOCs [49-53].

The diagnostic potential of exhaled breath is huge and has been applied to diagnose lung diseases, gastrointestinal diseases, metabolic disorders, renal diseases, liver

malfunction and others [4, 54]. Several different classes of compounds result from different process in the body.

Ketone bodies including acetoacetate and β-hydroxybutyrate are produced as a result of fatty acid metabolism. Acetone is formed by spontaneous decarboxylation of acetoacetate and through dehydrogenation of isopropanol [55]. It is very volatile and can be found in breath of all humans [56]. Acetone concentration is reported to increase in patients with uncontrolled diabetes mellitus [57-59].

Saturated hydrocarbons such are ethane and pentane are generated from lipid peroxidation of ω3 and ωa6 fatty acids by reactive oxygen species (ROS) [60]. ω3 and ωa6 fatty acids are components in cell membranes. Since, reactions of ROS and associated lipid peroxidation are the basis for inflammation [61], saturated hydrocarbons are found elevated during inflammatory events [62]. Ethane and pentane have been found elevated in several lung inflammatory diseases like asthma [63, 64], chronic obstructive pulmonary disease [65], pneumonia [66], acute respiratory distress syndrome [67] and obstructive sleep apnea [64].

Sulfur containing compounds result from incomplete metabolism of methionine in the transaminative pathway when mercaptanes are oxidized to sulfides [68]. During liver dysfunction, level of sulfur containing compounds like dimethyl sulfide, diethyldisulfides and ethyl mercaptane compounds elevate and give characteristic smell to patient's breath [69]. Elevations in sulfur containing compounds have been reported in blood and breath of patients with liver cirrhosis [69, 70]. Carbon disulfide seemingly generated as a

byproduct of methonine metabolism can act as an exhaled breath biomarker in lung transplant recipients with acute allograft rejection [71].

Nitric oxide (NO) is a ubiquitous gaseous free radical which plays a role in diverse physiological functions [72]. In the endothelium, nitric oxide functions in vascular signaling and is responsible for the activity of endothelium derived relaxing factor [73]. Released by pulmonary endothelium it mediates inflammatory responses and modulates airways smooth muscle contractility, pulmonary perfusion, and immune response [74, 75]. NO levels have been found elevated in the exhaled breath of asthmatic subjects [76-78]. Elevated NO in exhaled breath of asthma patients has been ascribed to constricted airways due to the activation of nitric oxide synthase 2A by damages to airway epithelial cells and/or by inflammation [79, 80]. This is helpful in differentiating asthma from other non-inflammatory lung disorders [81]. Exhaled NO has been used to distinguish healthy subjects with or without respiratory symptoms from patients with confirmed asthma [82, 83].Table 2.2 lists selected compounds found in breath, their potential origins and potential clinical applications.

With all the potentials and efforts in the field of breath analysis one would expect it to result in several robust procedures to be used as tests of clinical significance. Despite all the potential, due to inherent challenges of variability, lack of proper sample collection procedures, sample storage and intricate instrumental setups, the progress has been slow. Table 2.3 gives a list of tests that have been approved by US FDA for routine use in medical practice.

Table 2.2: Selected breath components, their potential origin and clinical applications

Compound	Source	Potential clinical application
Acetaldehyde	Ethanol metabolism	Monitoring of ethanol metabolism and oxidative stress
Acetone	Decarboxylation of acetoacetate, decarboxylation of isopropanol	Monitoring of diabetes and weight loss
Acetonitrile	Uptake of cigarette smoke	Monitoring of smoking behavior
Ammonia	Protein metabolism	End stage renal disease
Dimethyl sulfide	Liver failure	Monitoring Liver damage
Ethane	Lipid peroxidation product	Oxidative stress monitoring
Ethylene	Lipid peroxidation product	Oxidative stress monitoring
Isoprene	Cholesterol biosynthesis	Statin therapy monitoring
Malondialdehyde	Lipid peroxidation product	Oxidative stress monitoring
Methane	Gut bacteria	Gastrointestinal diseases
Propionaldehyde	Lipid peroxidation product	Oxidative stress monitoring
Propofol	Intravenous anesthetic	Monitoring of pharmacon during anesthesia
Trimethylamine	Uptake of trimethylamine or precursor	Monitoring of hemodialysis efficacy

Table 2.3: US FDA approved breath tests

Breath Test	Application	
Ethanol	Screening for blood alcohol	[84]
Nitric Oxide	Monitoring asthma therapy	[85]
Carbon dioxide (CO_2)	Capnography	[86]
Carbon monoxide (CO)	Neonate jaundice, CO poisoning	[87, 88]
$^{13}CO_2/^{12}CO_2$	Halicobactor pylori infection	[89]
Hydrogen	Lactose malabsorption	[90]
Alkanes	Grade 3 heart allograft rejection	[91]

2.2 Detection techniques for breath analysis

Though there are numerous gas detection techniques, to detect gaseous compounds at trace concentrations among hundreds of other gases and nearly saturated humidity with accuracy and precision required for medical diagnosis is challenging. Since breath is a complex matrix with components covering a wide dynamic range in concentration and diverse physical and chemical properties, numerous techniques have been utilized to analyze breath samples. Most important techniques in this field include gas chromatography coupled to mass spectrometric detection (GC-MS), selected ion flow tube mass spectrometry (SIFT-MS), proton transfer reaction mass spectrometry (PTR-MS), laser absorption spectroscopic techniques and chemical sensor. Though a detailed summary of each technique is beyond the scope of this chapter, a brief overview of few techniques used during the course of this thesis work is given in the following paragraphs.

GC-MS is the most traditional method for detection of trace gases in the breath. Many works reporting identities of different VOC's in breath have used the combination of gas chromatographic separation with mass spectrometric detection [3, 92, 93]. In GC, complex breath sample is injected into a chromatographic column. As the sample travels through the column by the flow of inert gaseous mobile phase, it is separated into components. This separation is based on property of the column that interacts with the sample. Non polar substrates in the GC column such as silicones separate the components according to their boiling points, whereas in a polar column the separation is determined by the polarity of the components [93]. This separation leads to different elution times for the components from the GC column. For a given analytical condition the elution times are compound specific and can be used for identification of the eluting components. Coupling of GC with MS analysis adds to its power. The eluting components are fed to ionization source leading to fragmentation patterns which are analyzed by a mass analyzer. The resulting mass spectra are characteristic of each component and can be used to identify the compound when compared to known fragmentation mass spectral patterns. Thus, MS provides an extra confirmation step to the previously identified compound based on the elution time. For quantification of a compound the GC instrument has to be calibrated with standard known concentrations of the pure compound. Solid phase microextraction (SPME) is commonly used for sample collection followed by automatic thermal desorption into the GC column. This approach, though improves the detection sensitivity, it compromises accuracy because of uncertainties in collection and desorption efficiencies. Also, because of the sample collection, feeding

and separation steps in the column and pre-concentration, GC-MS is not a real time measurement. Despite limitations GC-MS has been used in several earlier and recent studies [94-96] and has significantly contributed to our understanding of breath.

SIFT-MS is a relatively new analytical method to be applied to the field of breath research. It has its origins in the selected ion flow tube technique that was developed over thirty years ago for studying gas phase ion-neutral reactions occurring in interstellar clouds [97, 98]. It is now available as a tool suitable for online monitoring of breath samples in real time without the need for sample collection which is a significant advantage over GC-MS.

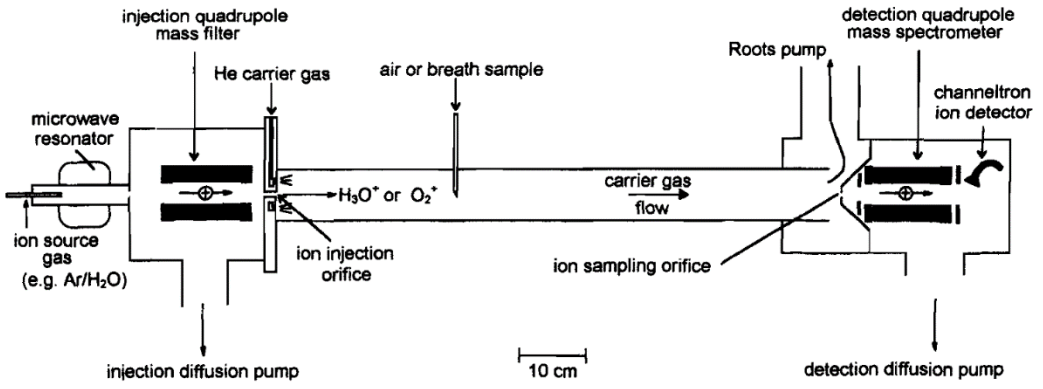

Figure 2.1: Schematic line diagram of SIFT-MS for analysis of trace gases in air or breath samples [1].

SIFT-MS utilizes the fast flow tube technique that allows ion-molecule reactions to proceed in a defined time period and facilitates accurate real time quantification of the analytes. Figure 2.1 shows a schematic diagram of a SIFT-MS instrument. A mixture of positive ions is generated in the microwave discharge ion source from ambient air and

humidity. Precursor ions based on their mass to charge ratio (m/z) are then chosen from this mixture using a quadrupole mass filter. Usually either H_3O^+, NO^+ or O_2^+ is chosen because none of them reacts with most common constituents (N_2, O_2, H_2O and CO_2) in the air but efficiently react with trace VOCs present. The selected ion which is called the precursor ion is injected in a flow tube with fast flowing inert carrier gas usually ultra-high purity helium at a pressure of about 100 Pa. The sample to be analyzed is also injected into the flow tube through a calibrated capillary at known flow rate. The precursor ions react with the sample to generate product ions. These precursor ions and the generated product ions are sampled through a pinhole orifice at the downstream end of the flow tube into a differentially pumped quadrupole mass spectrometer and ion counting system for analysis.

SIFT-MS has two modes of operation: 1) The full scan mode allows it to be used for detection and quantification of unknown compounds. 2) The multiple ion monitoring (MIM) mode for real time quantification of a known analyte in the sample. In full scan mode, a full mass spectrum is captured in a specified range of m/z values. The detection quadrupole is swept over the range in a chosen time while the sample is introduced into the flow tube. The height of each peak and the time is used to calculate the count rates. The spectra (Figure 2.2) is interpreted based on the knowledge of the ion chemistry involved between sample and the precursor ion. In MIM mode one or more specific compounds are chosen to be studied. The downstream quadrupole mass spectrometer is rapidly switched between the m/z values of the product ion, precursor ions and their

hydrated counterparts. MIM mode generates real time concentration profiles of selected compounds and water vapor (Figure 2.3).

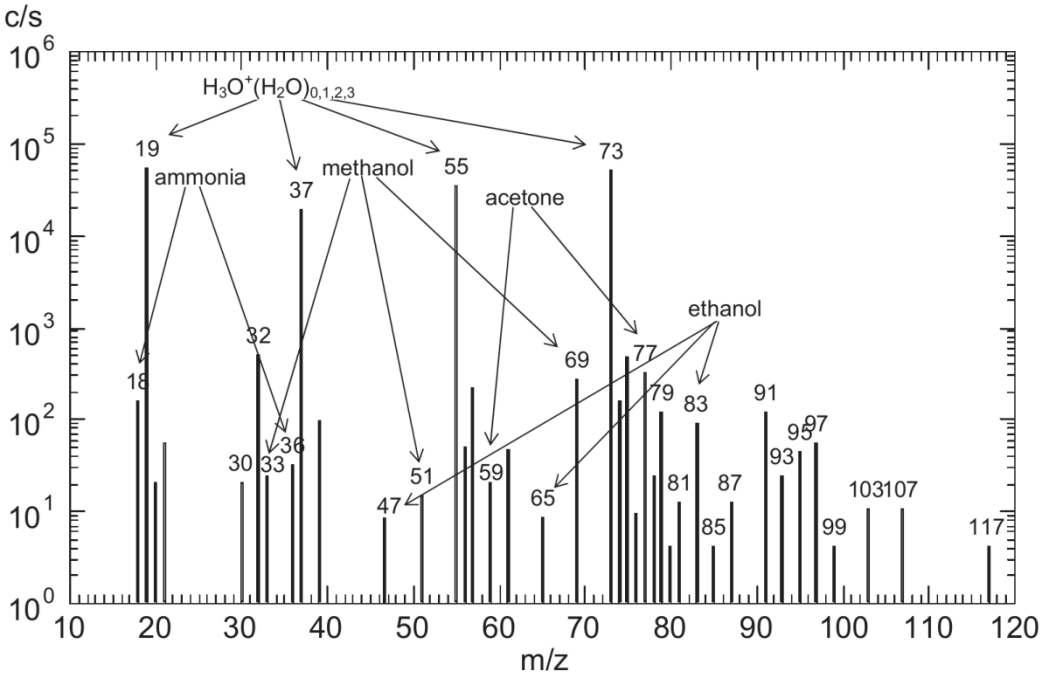

Figure 2.2: A typical SIFT-MS spectrum obtained in full scan mode. Counts per second (c/s) is plotted against *m/z* of the ions in the selected range of 10-120. H_3O^+ has been used as the precursor ion [2].

Accurate quantification of the compounds requires the reaction times and reaction rates to be known. Considering a hypothetical analyte A to be analyzed with H_3O^+ as the precursor ion, following reaction would occur

$$H_3O^+ + A \rightarrow AH^+ + H_2O$$

Generation of $AH^+$and loss of H_3O^+depends on the concentration of A in the carrier gas [A]. If k is the rate constant for the reaction then the concentration of product ions at time t is given by,

$$[AH^+]_t = [H_3O^+]k[A]t$$

The rate constant is accessible in the software for SIFT-MS analysis through an inbuilt library of rate constants. This library has been created and is constantly updated based on detailed SIFT studies of the reaction of various classes of compounds including alcohols, aldehydes, ketones and hydrocarbons with the three available precursor ions.

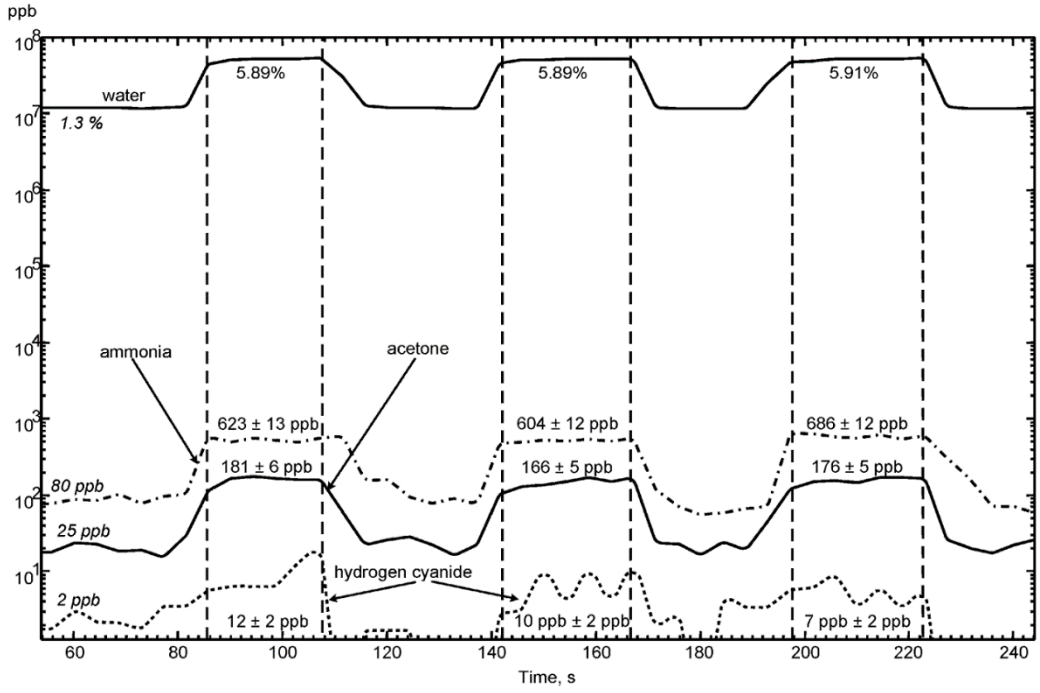

Figure 2.3: Time profile of concentrations obtained in MIM mode of SIFT-MS operation. Ammonia acetone, water vapors and hydrogen cyanide are simultaneously analyzed over three exhalations of breath.

With MIM mode and fast response time, SIFT-MS has been used for numerous breath sample studies. Subjects can directly breathe into the setup through a mouthpiece. To avoid condensation of humidity and blocking of the capillary, the sampling line is heated to about 100^{O}C. During the course of this thesis work, SIFT-MS has been used as

a standard detection method for acetone and water vapors in direct and conditioned breath samples.

Spectroscopic, including fluorescence and chemiluminescence based measurements are used for detection and quantification of specific compounds of interest in the breath. These methods are more suitable for studies involving already established breath markers or for monitoring identified and promising compounds. Nitric oxide is one such molecule which has been accepted as a marker for therapeutic monitoring of inflammation in asthma. During the work presented in chapter 3 on development of breath nitric oxide sensor, chemiluminescence based nitric oxide (NO) monitor has been used as the standard detection instrument. The detection is based on reaction of nitric oxide with ozone (O_3). This reaction results into production of nitrogen dioxide in the excited state.

$$NO + O_3 \rightarrow NO_2^* + O_2$$

$$NO_2^* \rightarrow NO_2 + h\nu$$

At reduced pressure, the excited nitrogen dioxide molecules emit radiations at wavelengths longer than 600 nm in red to near-infrared region of the spectrum [99]. These radiations are detected by a thermoelectrically cooled, red-sensitive photomultiplier tube. Since the ozone is generated in the instrument at a concentration of about 2% by volume, concentration of NO up to 500 ppmV can be measured. The detection limit for gas phase NO is about 0.5 ppbV. The advantage of these methods is that the detection is very specific, operation of the instrument and interpretation of the

data is relatively simple when compared to GC-MS or SIFT-MS. Spectroscopic methods have been employed to detect several compounds in breath including hydrogen peroxide [100], nitric oxide [101], carbon dioxide[102], acetylene [103], hydrogen sulfide [104] and acetone [105].

2.3 Portable device:

Though several studies related to breath biomarkers and their relevance to specific disease conditions have been reported, many analytical tools have been used to detect these biomarkers in exhaled breath, numerous potential sensor methods have been published, but still, portable breath sensor devices intended for en mass use are not available.

A portable breath sensor is warranted in modern health care where regular monitoring results in reduction of the ever growing burden of health care costs. Regular monitoring is not only necessary for managing clinical conditions as is done by blood glucose monitoring in case of diabetes but can also give early indication of the impending danger. However, regular monitoring is not so easy especially in free living conditions because of lack of easy to use devices, high cost per test and noncompliance from the users. It is best possible when the monitoring procedure is simple and painless, the cost per test is affordable, the data generated is processed, logged and can be analyzed with ease to track the user's personal record with minimal effort on the user's part to increase compliance. Breath analysis, of course, presents an easy to use and painless approach but still, affordable devices and low cost tests are not available.

Developing a solution to this effect requires a comprehensive approach where attention is paid not only to the detection technique but equal importance is given to every other component of the test like sample conditioning and delivery, individual variability, cost effective hardware, and smart compact device design. During the work presented in this thesis, sensors for exhaled nitric oxide and acetone have been developed. These gases are elevated in patients with asthma and diabetes respectively. Asthma and diabetes are among the top chronic conditions leading to hospitalization in US through emergency department [106].

Colorimetry has been chosen as the detection principle. Colorimetry is attractive because it results from strong specific interactions between molecules like formation of bonds, acid base interactions or charge transfer and π-π molecular complex formation. These strong interactions provide much needed specificity to detection towards a target molecule in the complex breath matrix consisting of thousands of interfering molecules in a wide concentration range. Many sensor approaches referred to as electronic noses have relied on van der Waal's interactions and physical adsorption which are much less specific. The detection is usually helped by use of pattern recognition algorithms on data generated by an array of surfaces available for interaction [107]. When these sensors are exposed to complex samples, especially moist samples like exhaled breath, the data interpretation can be difficult and complicated. So these sensors are at best qualitative and can be used for classification based on training through the data. Colorimetry is also attractive because given sufficient sensitivity of the color change, it allows for the use of

very cost effective and compact detection hardware like a digital camera or photodiodes supported by suitable data relay circuit for real time read out of the signal.

To truly achieve an affordable sensing solution, not only a cost effective hardware is required but low cost per test is also needed. For example commonly available blood ketone measurement devices based on electrochemical sensing principle cost around $15 may sound reasonable in US but they still need a measurement strip which costs around $7 for each test. If a patient needs to monitor her/his blood ketone levels regularly on a daily basis or multiple times a day then the costs will mount up and the measurement is no longer easily affordable. This would mean that the most frequently replaced component does become a limiting factor for the use of the device. Keeping this in mind, replaceable sensor cartridge which houses the color changing chemicals for the developed colorimetric sensors have been carefully optimized on very low cost cellulose paper coated with nanoporous alumina or silica for increased sensitivity. The hardware for sample delivery has been kept minimal by either using miniature pumps in case of the nitric oxide sensor or without the pump in case of the acetone sensor. For sample conditioning of the humid sample, optimized amounts of calcium chloride after numerical simulation of desiccation process have been used. The overall aim has been to develop and integrate approaches that focus on functioning of the device in real scenario with minimal cost and effort to the user.

Wireless data transmission capabilities, processing and presentation of the data on smartphone devices and compact housing for the hardware have been developed by other

members of the lab at the Center for Bioelectronics and Biosensors at the Biodesign Institute, ASU.

3

SENSOR FOR EXHALED NITRIC OXIDE

3.1 Introduction

Exhaled human breath consists of several gases including nitric oxide (NO) in ppbV range [108]. Endogenously, nitric oxide is generated by three isoenzymes of NO synthase (NOS). Isoforms I (NOS1) and 3 (NOS3) are constitutive forms and play regulatory roles such as neurotransmission and regulation of local blood flow. Isoform 2 (NOS2) which is the inducible form of NOS, is not constitutively expressed but is induced by stimuli resulting from inflammation and infections. The large amount of NO produced by NOS2 may have proinflammatory effect. In case of inflammatory airway diseases such as asthma, exhaled nitric oxide has been found to increase mainly because of inducible NOS2.

Asthma is a chronic respiratory disease that affects 235 million people worldwide including 18.9 million adults and 7 million children in United States alone [109-111]. According to the National Asthma Education and Prevention Program Expert Panel [112] from the US National Institutes of Health, "Asthma is a common chronic disorder of the airways that is complex and characterized by variable and recurring symptoms, airflow obstruction, bronchial hyper responsiveness, and an underlying inflammation. The interaction of these features of asthma determines the clinical manifestations and severity of asthma and the response to treatment." Because of the complexity of asthma, the pathogenic mechanisms leading to the condition may be several. In addition, patient's response to different therapies is not uniform, nor is it necessarily consistent in individual

patients over time. Though the underlying causes and the responses to therapies may vary, the vast majority of these worsening are associated with increased levels of airway inflammation. Consequently, analytical measurement of airway inflammation in asthma could be of significant importance. Such measurements could inform the proper choice of therapy and help to avoid medication overdoses. The most direct measures of airway inflammation, however, are too invasive and have limited clinical use. Bronchial biopsy which is considered to be the gold standard of assessing airway inflammation is expensive, invasive and technically complex.

The level of exhaled nitric oxide (eNO) in asthmatic patients is elevated [78, 113]. This elevation is associated with increased expression of inducible NOS2 which is sensitive to corticosteroids [80, 114-116]. Further studies show exhaled nitric oxide's association with allergen induced airway inflammation [117-119]. eNO also correlates well with inflammatory markers in bronchial biopsy, broncho-alveolar lavage and induced sputum analysis [117, 120-122]. These studies have established eNO as a standardized noninvasive biomarker that evaluates airway inflammation in asthma [77, 123-125]. Its utility to assess response to anti-inflammatory therapy has also been well studied [126, 127].

Since the detection of NO in exhaled breath in 1991 by chemiluminescence, diazotization and mass spectrometry [108], efforts were made to develop sensitive and simpler nitric oxide analyzers. The most commonly used gold standard method is based on chemiluminescence which has been commercialized for breath analysis. For example NOA280i (Severs, GE Analytical Instruments, Boulder, USA), Analyzer CLD 88sp

(ECO MEDICS, Duernten, Switzerland) and NA623N (Chest, MI, Tokyo, Japan). NOA280i has been used as the reference standard method for NO detection in the work presented in this chapter. The instrument can be used for both online and offline measurement of exhaled nitric oxide. Measurement of eNO is critically dependent on expiratory flow rate [128, 129]. Also, NO levels in dead space air and nasal cavity are high [130, 131]. Therefore, a standardized method to sample eNO is needed. Such standardized methods have been recommended by international guidelines for sampling and measuring eNO both in adults and children [132-135].

Considering the value of monitoring eNO for personalized asthma management, low cost and portable solutions would better serve patients and clinicians. For this, several platforms have been explored. Commercial systems based on electrochemical detection which are more compact and portable than the chemiluminescence method are available. For example, NIOX MINO (Aerocrine, Stockholm, Sweden) and NObreath (Bedfont Scientific, Kent, UK). These sensors still cost a few thousand dollars. Also, they suffer from non-uniform calibration issues and show deviations in correlation [136, 137]. Despite these issues they still present a step forward towards a solution for clinicians. The sensor presented in this chapter aims to reach the goals of being a portable, low cost and easy to use device which can be afforded and used not only by clinicians but also by patients to manage their conditions at a personal level.

3.2 Detection principle and setup

The detection principle used to detect nitric oxide was based on colorimetric change of chemical probe on exposure to nitrogen dioxide [138]. Exhaled breath sample

was conditioned through an oxidation tube which provided the only source of nitrogen dioxide for reaction with the probe. Figure 3.1 shows visible spectrophotometric changes of the molecular probe, o-phenylenediamine upon reaction with nitrogen dioxide. Increase of absorbance in the range of 350-550 nm observed in the figure formed the basis of the sensing mechanism.

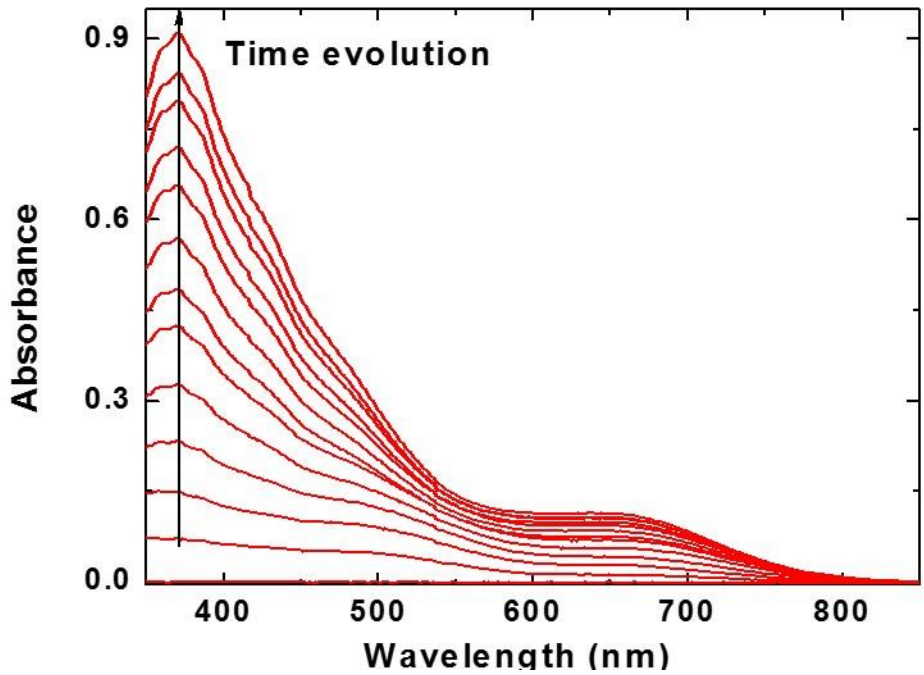

Figure 3.1: UV-visible spectrum of o-phenylenediamine upon reaction with 10 ppmV NO_2

For detection of the color development, a sensing platform was developed which consisted of a complementary semiconductor metal oxide (CMOS) imager as optical detector which was controlled by a software program developed in the Center for Bioelectronics and Biosensors at the Biodesign Institute. The imager captured real time intensity at an acquisition rate of 5 Hz from two different elements. One of the element

acted as a sensor and the other as a reference (Figure 3.2). The reference was devoid of the colorimetric probe. So, upon exposure to the sample it did not result in color change but correlated with intensity changes due to other factors including scattering, changes in the light source or noise in the detection circuit. This allowed for correction of these factors in the signal from the sensing region. The logarithmic ratio between the sensing and the reference elements was evaluated as the output signal. This signal corresponded to absorbance change due to the reaction and was directly proportional to the concentration of the analyte, nitric oxide in this case.

$$\Delta\, Absorbance = -\log\left(\frac{I_{sensing}(t)}{I_{reference}(t)}\right) - constant \quad \text{(i)}$$

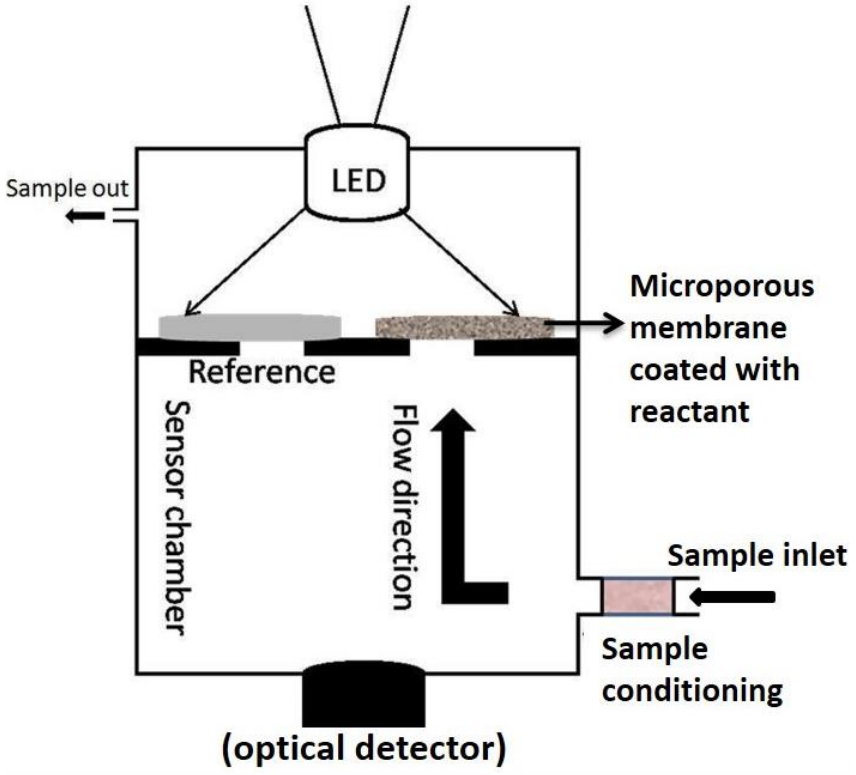

Figure 3.2: Schematic representation of the NO sensing platform.

Figure 3.3 (A) shows the intensity value captured by the imager from the two elements. Both the regions were purged with clean air for the first minute. In this duration the intensity was nearly constant with slight drift due to flow on both the elements. For the next two minutes nitrogen dioxide was sampled which resulted in a linear decrease in the intensity on the sensing element due to color development. The reference element was not affected by the introduction of the sample. The system was again purged for the next minute. In this duration the color development stopped and both sensing and reference elements went back to a constant intensity with flow drift.

The intensity data was transformed to change in absorbance as shown in Figure 3.3(B) using equation (1). The absorbance change increased linearly with time. The sensitivity of detection could be optimized by adjusting the sample injection time.

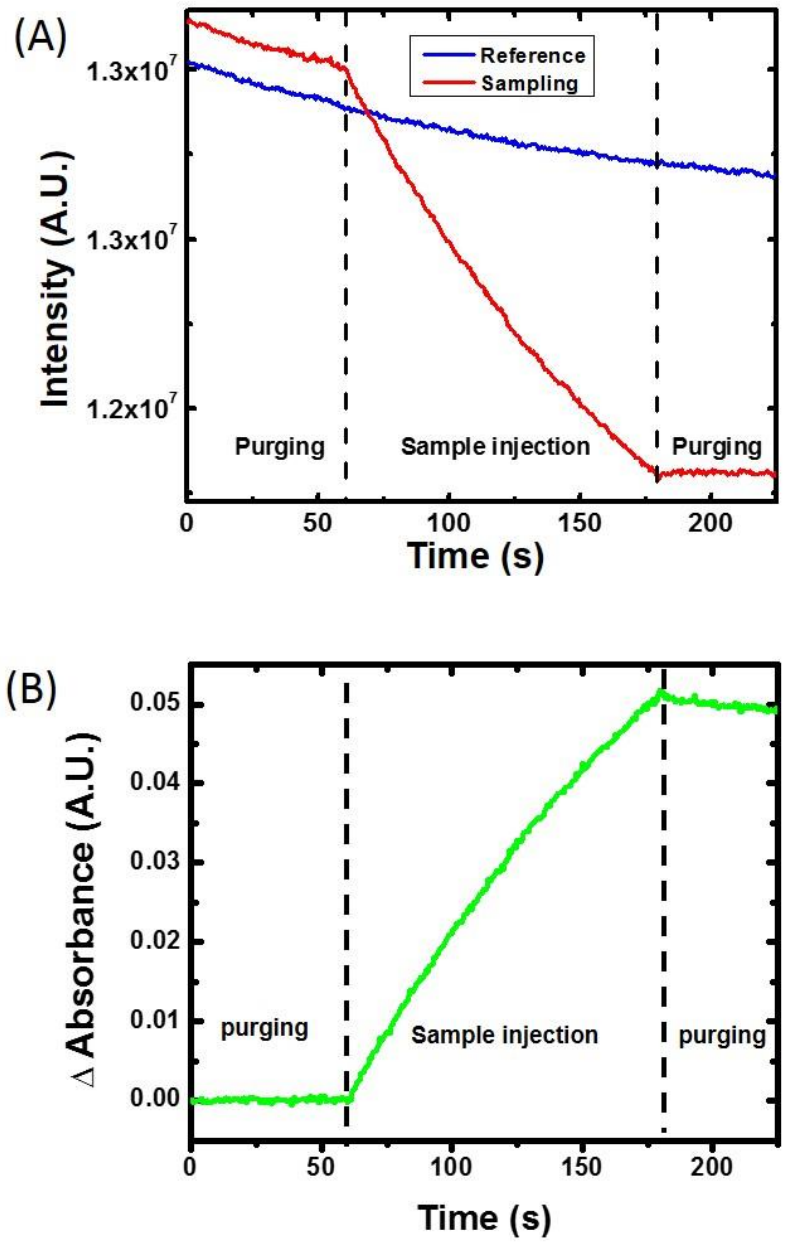

Figure 3.3: (A) Transmitted intensity of light recorded by the optical imager from the reference and sensing elements during NO_2 measurement. The injection of 50 ppbV NO_2 sample was preceded and followed by air purging for baseline collection. (B) The observed intensity data converted to change in absorbance (-log (sensing intensity/reference intensity) - constant). This signal was proportional to concentration of NO_2 in the sample.

The developed detection setup was simple and compact allowing for a low cost and portable device (Figure 3.4). The sensor material was low cost and highly sensitive due to the support matrix. The support matrix provided (1) an excellent host for high surface concentration of the molecular probes, enabling a high dynamic detection range and lifetime, (2) a good medium for quick diffusion and transport of nitrogen dioxide, (3) a medium that promoted the formation of colored products and (4) a highly stable support for the sensor for several months.

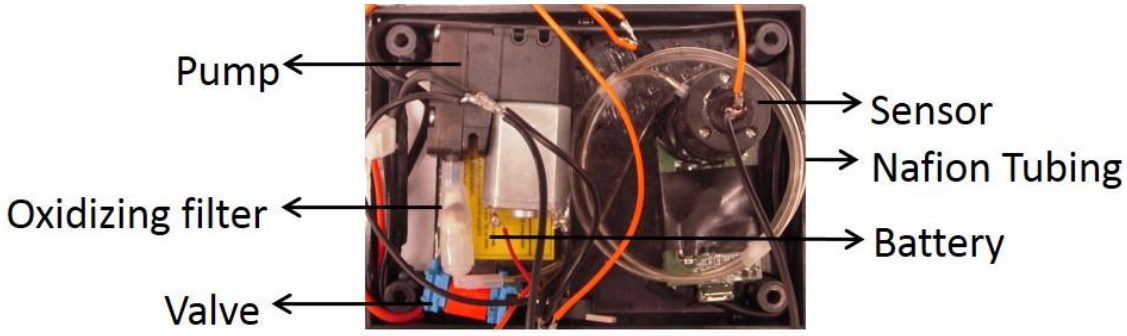

Figure 3.4: Sensor prototype implemented with white LED as the light source and a 2 megapixel web camera as the imager.

3.3 Experimental

3.3.1 Standard gas samples

All optimizations were performed with standard nitrogen dioxide (50 ppmV in nitrogen) and standard nitric oxide (50 ppmV in nitrogen) gases from Praxair Inc. The testing concentrations of these gases were prepared in tedlar bags (Custom Sensor Solutions Inc.) by dilution with humidified air (Ultra Zero; Air Liquide). The

concentration of the prepared bags were measured by a reference chemiluminescence detector.

3.3.2 Collection of breath samples

Breath samples were collected in tedlar bags by blowing into the bag through a barometric valve against a constant pressure of 12 cm water at room temperature. Before blowing into the bags, the inhalation was done through a particle filter and initial 150-200 mL of the sample was discarded.

3.3.3 Reaction product characterization

High Performance Liquid Chromatography/Mass Spectrometry (HPLC-MS) was used to characterize the reaction products. Two sensing elements (Control A and Sensing element B) were treated according to the following protocol:

Control A: A sensing membrane prepared with o-phenylenediamine was dipped in 2 mL of acetonitrile (HPLC grade) and was shaken for 5 min. After this, the liquid extract was centrifuged and the supernatant was injected into a HPLC for separation and collection of the separation products. The main product fraction was analyzed by MALDI-TOF mass spectrometer.

Sensing element B: A sensing membrane prepared with o-phenylenediamine was used to test a high NO_2 concentration (1 ppmV) for a long period of time until a clear color development was visually observed. Then, the sensing element was dipped in 2 mL of acetonitrile (HPLC grade) and mildly shaken for 5 min. The liquid extract was centrifuged and the supernatant was injected into a HPLC. The separated products were

collected, and the main product fraction was analyzed by MALDI-TOF mass spectrometer.

3.4 Results

3.4.1 Sensor response

The sensor showed a linear time response to nitric oxide injection as shown in Figure 3.5. Nitric oxide sample at a concentration of 50 ppbV was injected for 20 s after 30 s of purging with humidified air. The system was again purged for 20 s following sample injection. The setup had a low baseline noise level of $5x10^{-5}$ absorbance units. At this noise level, the detection limit of 0.4 ppbV was achieved. The advantage of this sensitive response was that the time of detection could be as low as 5 s for detection in clinically relevant range of NO concentration.

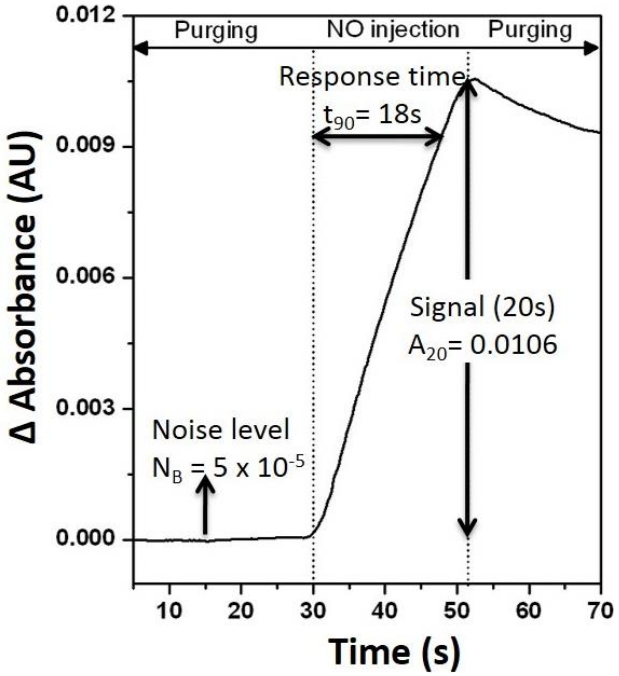

Figure 3.5: Sensor response to 50 ppbV NO.

3.4.2 Sensor optimization

The molar extinction coefficient of the reaction product was estimated by fitting the peak absorbance data (Figure 3.6) obtained by reacting 1 mM o-phenylenediamine solution with nitrogen dioxide on a pseudo first order kinetic model.

$$A = \alpha\left(1 - e^{-\beta t}\right) \qquad (1)$$

$$\varepsilon = \frac{\alpha}{C_0} = 1.5 \times 10^2\ M^{-1}.cm^{-1} \qquad (2)$$

Here, A was the absorbance, α and β were fitting parameters, ε was the molar extinction coefficient and C_0 was the initial concentration of o-phenylenediamine. The calculated molar extinction coefficient of $1.5x10^2$ $M^{-1}.cm^{-1}$ was about an order of magnitude lower compared to other regular colorimetric dyes. Thus, the sensor had to be optimized for maximum capture of the analyte gas. Alumina coating was used for this purpose with provided an increased surface area improving the sensitivity of detection by a factor of 2.5 as shown in Figure 3.7. The capture efficiency of the gas was estimated to be 93% by measuring the concentration of the inlet and outlet sample and taking the ratio of gas consumed to the amount of gas introduced.

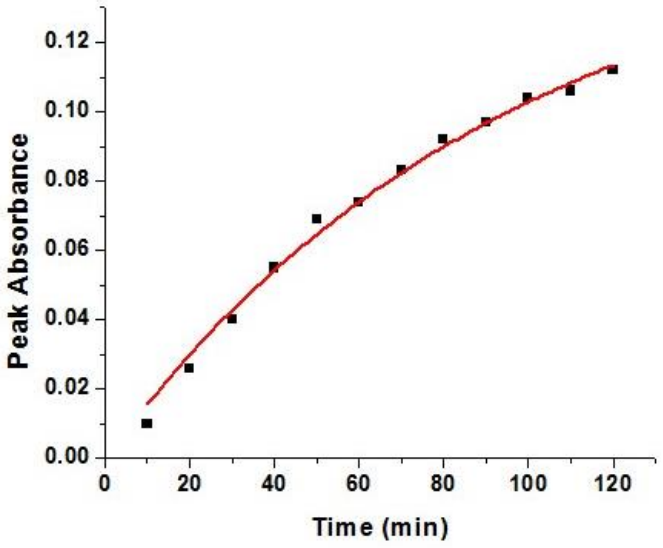

Figure 3.6: Peak absorbance data collected over time with gaseous NO_2 reacting with 1mM o-phenylenediamine. The data is fitter on pseudo liner kinetic model $A = \alpha (1-e^{-\beta t})$.

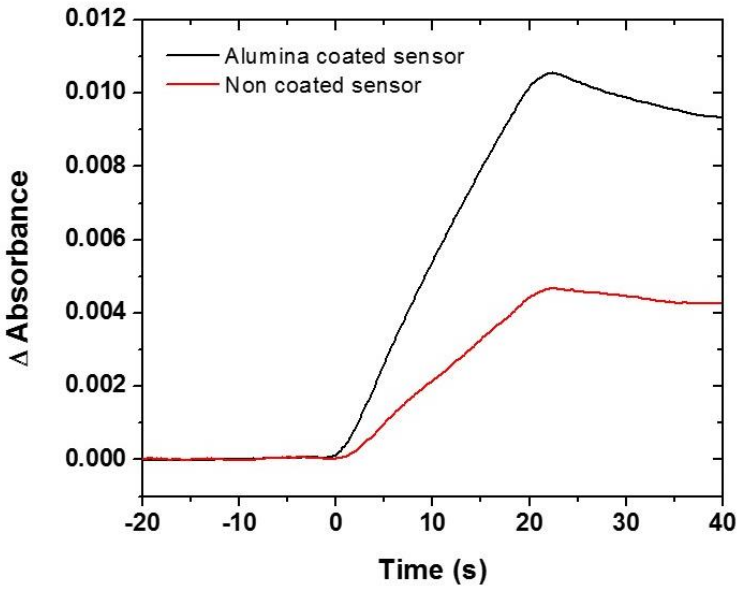

Figure 3.7: Detection of 50 ppbV NO with cellulose sensing element without alumina treatment and after alumina treatment. The signal improved by a factor of 2.5 after alumina treatment of the cellulose membranes.

The sensors were tested for reproducibility of detection for a single injection and also over multiple injections on the same sensor. Figure 3.8 shows 16 consecutive injections of 35 ppbV NO separated by a short purging time with a variation of 7%. Figure 3.9 shows response of 29 different sensors towards 50 ppbV NO. The mean detected concentration was 50.43 ppbV with a variation of 6.5%.

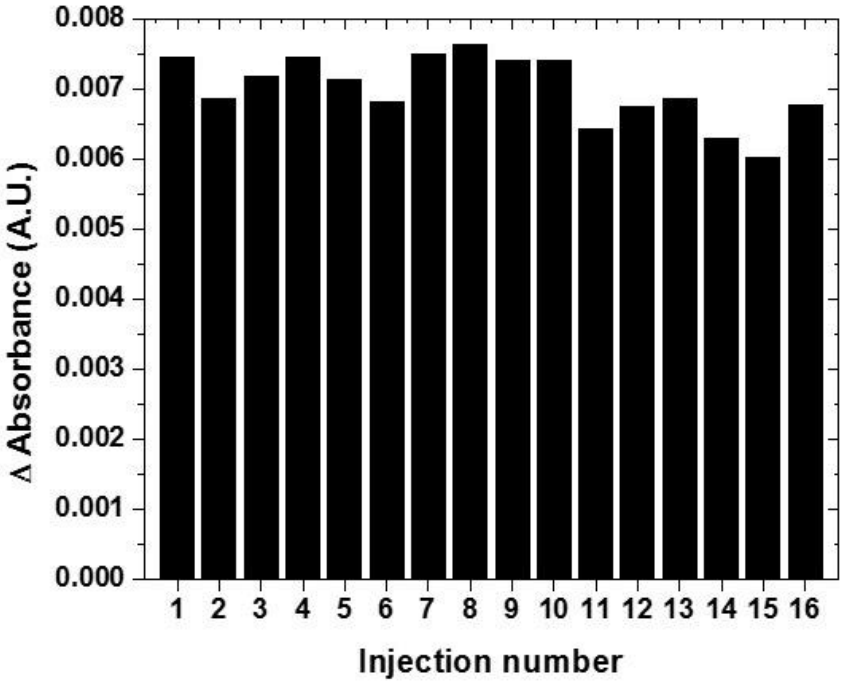

Figure 3.8: Change in absorbance measured over 16 consecutive injections of 35 ppbV NO on a signal sensing element. Injections were separated by a short purge time. The coefficient of variation was 7%.

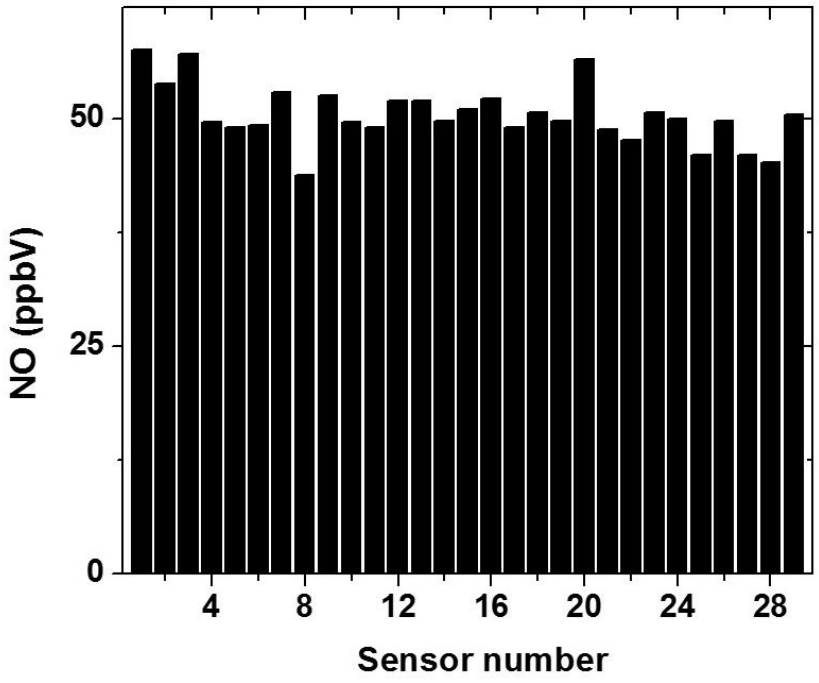

Figure 3.9: Detection of 50 ppbV NO on 29 different sensors. The mean detected concentration was 50.43 ppbV and coefficient of variation was 6.5%.

3.4.3 Mass transport study

The response of the sensor was characterized as a function of sample flow rate. The flow was restricted to values achievable with a miniature pump used in the portable device. A linear dependence of the response on the flow rate was found as shown in Figure 3.10 indicating mass transport controlled response of the sensor. To maximize the sensitivity a flow rate of 450 $ml.min^{-1}$ was used in this work.

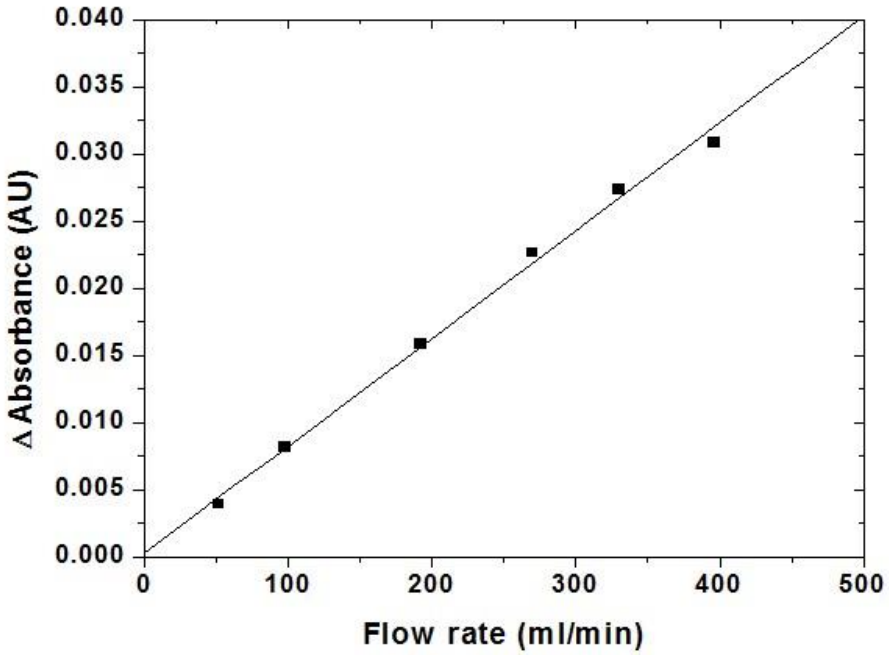

Figure 3.10: Response of the sensor to 200 ppbV NO_2 at different sample flow rates achieved using miniature pumps. Injection time was 20 s.

3.4.4 Sensor calibration and correlation

The sensor was calibrated in the clinically relevant range of 5-200 ppbV NO using standard gas. The response to NO concentration was linear as shown in Figure 3.11 with a correlation coefficient of 0.996 and slope 4.9×10^{-5}. The error bars represented the standard deviation of six measurements for each concentration.

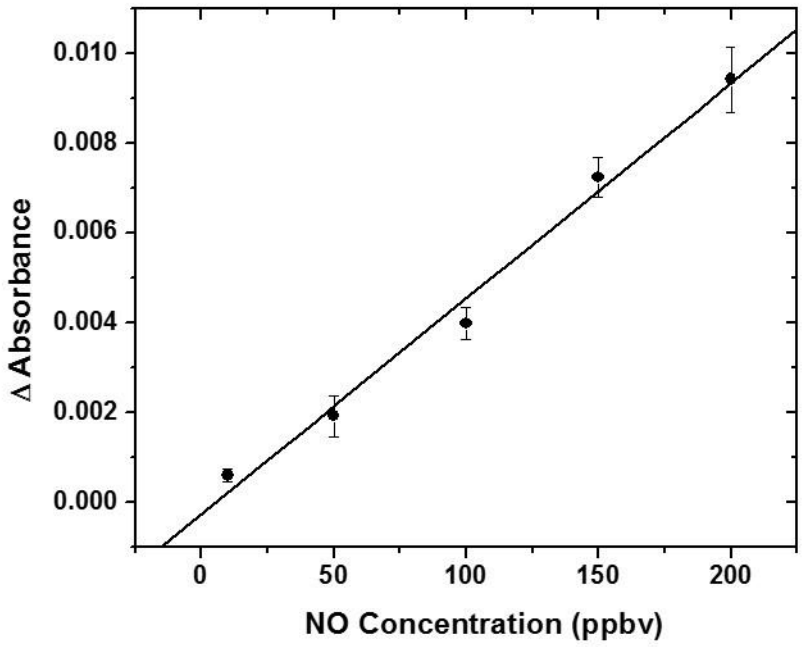

Figure 3.11: Sensor calibration curve. Standard NO gas was used and reference measurements were done with chemiluminescence based NO analyzer.

NO concentration in breath samples were measured offline after collection of the samples in tedlar bags according to the guideline provided by ATS. Figure 3.12 shows a correlation plot of the measurements done with the developed sensor versus the concentrations measured with the gold standard chemiluminescence method. The breath samples were collected and then the same sample bag was tested with the chemiluminescence method followed by the developed sensor. The slope of the correlation plot was 0.9.

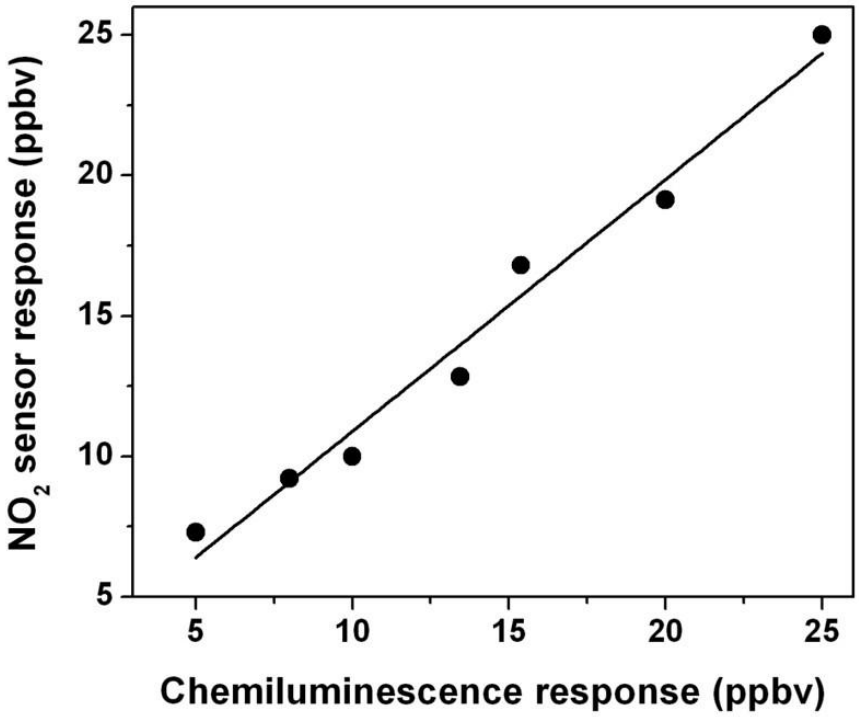

Figure 3.12: Correlation of the developed colorimetric sensor with the gold standard chemiluminescence detection. Slope was 0.9.

3.4.5 Selectivity of detection

The selectivity of the sensor was evaluated by measuring its response towards several compounds commonly found in human breath and the environment. Given the low response of the molecular probe to these interfering gases, tests for selectivity were carried out at much higher concentration of the interfering gases than regularly found in human breath or the environment. The selectivity coefficient was calculated as the ratio of sensor response to nitric oxide and to the interfering gas at the same concentration. Table 3.1 lists the selectivity coefficient for several interfering gases. There was no significant effect on the signal of these gases at their commonly found concentrations in

the breath. However, the sensor showed a selectivity coefficient of 0.9 towards ozone which is an environmental pollutant. Considering that human breath is devoid of ozone and the sensor sampling time to be small, the possible effect of environmental ozone was not an interference concern. Though, in order to use the sensor for environmental monitoring, ozone scrubber based on molybdenum oxide derivative (2B Technologies, Bouler, CO) was successfully integrated to remove ozone from the sampling line [139].

Table 3.1: Selectivity of the NO_2 test with o-phenylenediamne over possible interfering gases.

Compound	Selectivity coefficient
SO_2	6.1×10^4
CO	3.1×10^5
CO_2	1.5×10^7
NH_3	1.3×10^4
H_2S	1.7×10^4
Acetone	4.5×10^4
Ethanol	5.6×10^4
Ozone	0.9

3.4.6 Sensor stability

A batch of several sensing elements was prepared and stored at ambient temperature in a clean nitrogen atmosphere to test their stability. After different periods of time, a sensor was taken out from the storage and tested against 50 ppbV of standard NO_2 sample. The response of the sensor was tested for a period of 4 months with a variation of 10% as shown in Figure 3.13.

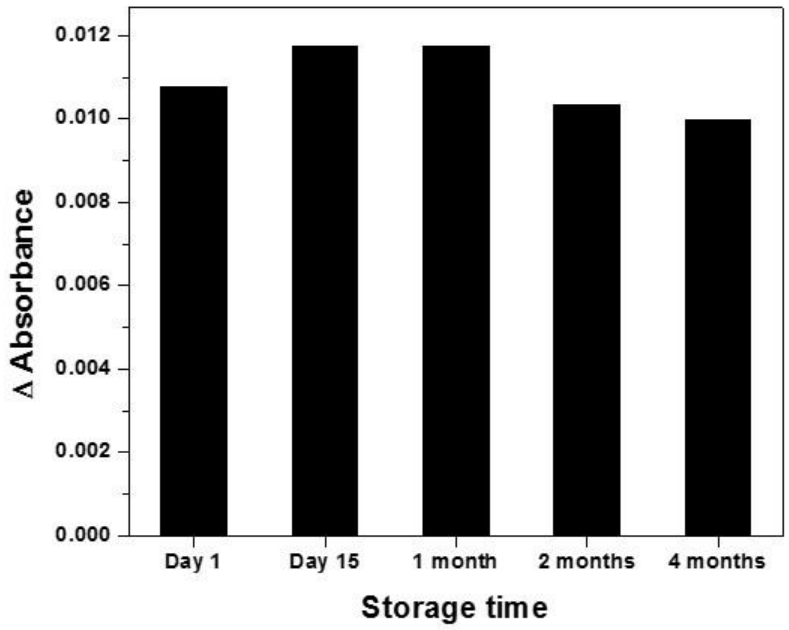

Figure 3.13: Response of different sensing elements prepared in one batch and stored at room temperature in a nitrogen atmosphere. Tests were performed with 50 ppbV NO_2 samples.

3.4.7 Reaction product characterization

Figure 3.14 shows the mass spectrum obtained from the HPLC separated component from the reference control and sensing elements. It was clear that the main

compound in control (before the reaction with NO_2) corresponded to o-phenylenediamine with a molecular weight of 108 a.m.u, and that the main product after the reaction in sensing element had a molecular weight of 211 a.m.u.

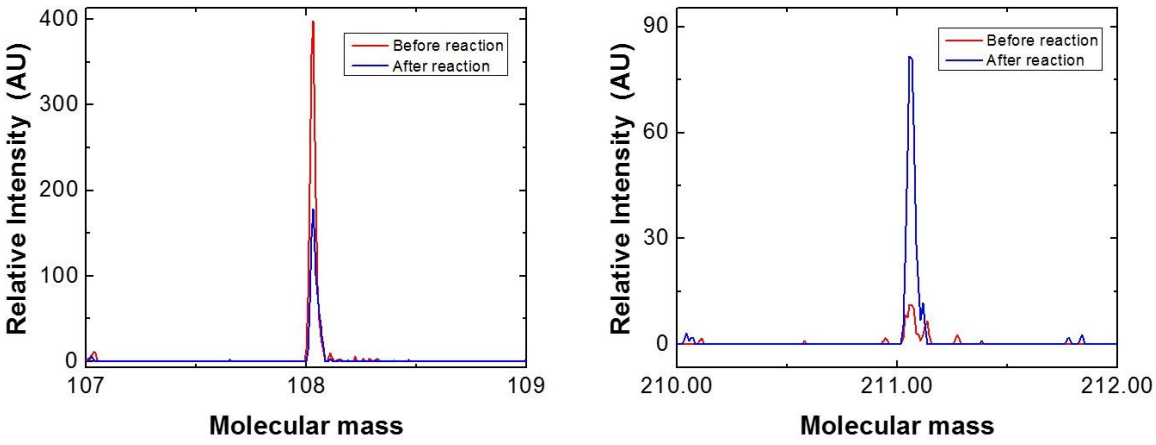

Figure 3.14: Mass spectra from MALDI-TOF analysis of HPLC separated component corresponding to the main product in control (Red) and sensing (Blue) elements before and after the reaction with 1 ppmV NO_2.

3.5 Conclusions

In summary, a working sensor prototype for the measurement of eNO based on oxidation of NO to NO_2 followed by colorimetric reaction and detection has been developed. All components of the chemical sensor, detection setup and sample delivery have been carefully optimized to achieve ulrasensitive detection. The measurement of nitric oxide concentrations in the clinically relevant concentration range with high sensitivity, precision and quick response time has been demonstrated. The instrument has advantages of being portable, cost effective and simple in operation compared to

currently used eNO detectors. The instrument holds promise for giving the clinicians and patients an affordable tool for better management of asthma.

4

ONLINE SAMPLE CONDITIONING FOR PORTABLE BREATH ANALYZERS

4.1 Introduction

To be relevant as a solution, a sensor has to be capable of working in the real world. For this, all process till the end detection need to be efficiently working. Even though several sensor publications present new chemical detection methodologies sample collection and conditioning that often determine whether a sensor can work in real world, are much less emphasized. This is especially the case for breath analyzers where sample conditioning presents a significant challenge. It is even more difficult in a portable breath analyzer with limited hardware and size constrains. Human breath is nearly saturated with water vapor (>95% RH) [140, 141] which coming out at body temperature condenses in the sensor. This causes several problems including blockage of sampling lines, pre-concentration of unwanted analytes and noise due to unpredictable changes in detection properties like mass, conductivity or optical transmission and often leads to the failure of the breath analyzer. For proper functioning a breath analyzer requires proper sample conditioning before detection [101, 142].

A solution commonly employed to condition high humidity in the breath sample is introduction of nafion tubing in the sampling line to reduce humidity. However, the reported efficiencies of humidity reduction by nafion tubing are highly variable, ranging from 58% to 98% depending on ambient humidity [143, 144]. For this reason many applications must flow additional drying gas into the nafion tubing in order to maintain the efficiency [145], which adds complexity into the device, and also makes it unsuitable

for a portable breath analyzer for personal monitoring. A more serious issue with the nafion approach is that it removes not only unwanted humidity, but also partially or completely (75% to >90%) remove many wanted analytes, such as low-molecular-weight, polar, oxygenated compounds, including some ketones, alcohols, aldehydes, and water-soluble ethers [143]. These analytes are of high clinical significance for different diseases. Real time breath sample measurement without removal of humidity has been done using mass spectrometric platforms including selected ion flow tube (SIFT) [146, 147] and proton transfer reaction (PTR) [50, 148, 149] mass spectrometry. These techniques employ special handling of breath sample to avoid humidity condensation and require long heated tubes and capillaries heated up to 100 ^{o}C [51, 150, 151]. In addition to conditioning the humidity of a breath sample, another critical requirement for breath analyzer is to provide an appropriate volumetric flow rate and back pressure. The flow rate and back pressure requirements differ depending on specific guidelines for the analyte being measured. For example, in the case of breath nitric oxide, a biomarker for inflammation, the American Thoracic Society, recommends that the back pressure should be at least 5 cm H_2O [152].

This chapter outlines an effort to overcome the difficulties discussed above. The results have been published in scientific journal [153] where a breath sample conditioning approach is presented which is based on desiccant particles packed in tubing. The tubing can be integrated into the inlet of existing breath monitoring devices. The relationships of the output humidity, flow rate and pressure in terms of controllable parameters, such as particle size and tubing geometry is developed. The relationships are established based on

numerical simulation and validated experimentally. Using this approach, mouthpieces have been designed and used for nitric oxide detection using a hand held device developed during the work presented in chapter 3 [138].

4.2 Experimental and Simulation Methods

4.2.1 Simulation methods

Numerical simulation of the desiccation process in the mouthpiece was performed using finite element method software COMSOL multiphysics 3.5. The simulation included models for flow and mass transport in the porous medium of calcium chloride, which was used as a desiccant material to adsorb water and control humidity. Temperature change during the desiccation process was not taken into account for simplifying the model. It was experimentally observed that the temperature increased by about 20 ^{o}C at the mouthpiece inlet for 1 L of breath sample whereas the outlet temperatures increased by 1-2 ^{o}C. This rise in temperate did not have considerable effect on the working efficiency of the overall desiccant tube (Table 2) since enough material in the tube was far away from saturation. A 2-dimensional rectangular geometry with rotational symmetry, as shown in Figure 4.1, was used to simulate the cylindrical tubing. The tubing, defined as a subdomain, was packed with the desiccant particles of different diameters (d) into a porous structure, with porosity, ε_p, varying from 0.25 to 0.65. The permeability (κ) of the system for a given porosity and particle size was estimated by Kozeny's relation [154],

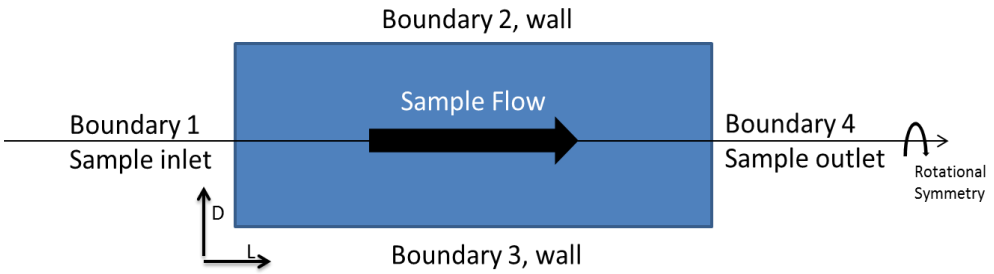

Figure 4.1: Representation of the modeling domain of the cylindrical desiccation tube in two dimensions assuming a rotational symmetry of packing.

$$\kappa = \text{constant} \times \frac{d^2 \varepsilon_p^3}{(1-\varepsilon_p)^2} \qquad (4.1)$$

The constant in the equation was determined experimentally to be 984 by measuring the sample flow rate (v) and pressure difference across a known length (Δx) of the mouthpiece using Darcy's law [155],

$$v = \frac{\kappa}{\eta} \frac{\Delta P}{\Delta x}, \qquad (4.2)$$

where η is the dynamic viscosity (1.74×10^{-5} Pa.s) of humid air at physiological temperature [156].

Brinkman equations given by

$$\frac{\rho}{\varepsilon_p} \frac{\partial \boldsymbol{u}}{\partial t} + \nabla \cdot \left[-\frac{\eta}{\varepsilon_p} (\nabla \boldsymbol{u} + (\nabla \boldsymbol{u})^T) + p\boldsymbol{I} \right] = -\frac{\eta}{\kappa} \boldsymbol{u} \qquad (4.3),$$

$$\boldsymbol{\nabla} \cdot \boldsymbol{u} = 0 \qquad (4.4)$$

were used to model the flow of breath through this medium, where, ρ denotes the density of humid air (1.15 $Kg.m^{-3}$) and, u represents the velocity, and p refers to the pressure.

Equation 4 above implies that the fluid flow is incompressible in the subdomain. Since Mach number for the flow at 6.67 L.min^{-1} through a typical mouthpiece geometry is less than 0.3, the only appreciable fluid density change resulted from change in temperature of the breath due to rise in desiccant temperature. The increase in breath temperature was measured to be less than 3 ^{o}C resulting in ~1% increase in density for which the assumption of incompressible flow is valid. Boundary conditions for the flow were set as follows,

Boundary 1: $\boldsymbol{u} \cdot \boldsymbol{n} = u0$ (inlet), where u0 is the linear flow velocity at the inlet;

Boundary 2 and Boundary 3: $\boldsymbol{u} = 0$ (wall);

Boundary 4: $p = 0$ (outlet).

With these subdomain and boundary settings, the velocity field was determined and the solution obtained was further used to solve the mass transport process using COMSOL 3.5.

Mass transport of water within the desiccant tube was described by the diffusion-convection equations,

$$\frac{\partial C_i}{\partial t} + \nabla \cdot (D_i \nabla C_i + C_i \boldsymbol{u}_i) = R\,, \qquad (4.5)$$

where C_i denotes the concentration of the species, D is the diffusion coefficient, u represents the velocity and R refers to the rate of consumption of species i. These equations were applied to the two components of the desiccation process viz. humidity in the breath (i=1) and the surface binding sites available on desiccant calcium chloride for

capture of humidity (i=2). For breath, the diffusion coefficient of water vapor was set to be 4.6×10^{-7} $m^2.s^{-1}$ [157]. The boundary conditions were set as follows,

Boundary 1: $C_1 = C_1^{in}\left(1 - e^{-\frac{t}{2}}\right)$ (inlet, allows humidity to rise from 0 to within 1% of the maximum breath humidity C_1^{in} in 10 s compensating for time lag due to sampling of non-alveolar dead space air),

Boundary 2 and Boundary 3: $n \cdot (D\nabla C_1 + C_1 u) = 0$ (wall), and

Boundary 4: $n \cdot (D\nabla C_1) = 0$ (outlet, no convective flux).

For binding sites on the solid calcium chloride, diffusion was neglected and all the boundaries were set as wall for mass transfer [i.e. $n \cdot (D\nabla C_2 + C_2 u) = 0$] assuming no inflow or outflow of the desiccant material through any boundary. The rate of water vapor consumption was given by the linear driving force approximation [158-160],

$$R = k_0 (C^* - C^s), \quad (7)$$

where, k_0 is mass transfer coefficient, obtained from parameter fitting to be 5.5×10^{-3} s^{-1}, C_s represents the surface concentration of water on the calcium chloride surface at any given time and C* is its equilibrium value. Equilibrium water concentration was modeled through Dubinin-Astakhov equation approximated as [161-163],

$$C^* = \frac{C_2^0 k_1 C_1}{1 + k_2 C_1} \quad , \quad (8)$$

where, C_2^0 represented the initial concentration of binding sites on calcium chloride available for humidity capture. k_1 and k_2 were equilibrium parameters obtained from

fitting, which were 0.33 $m^3.mole^{-1}$ and 0.01 $m^3.mole^{-1}$, respectively. The surface humidity concentration at any time was represented as,

$$C^s = C_2^0 - C_2 . \qquad (9)$$

Finally the rate of consumption was obtained as

$$R = k_0 \left[\frac{C_2^0 * k_1 C_1}{1 + k_2 C_1} - \left(C_2^0 - C_2 \right) \right] . \qquad (10)$$

These mass balance equations with the appropriate boundary conditions described above were solved using COMSOL 3.5 coupled with the velocity field obtained earlier with the flow simulation to generate concentration profile of breath humidity introduced into the desiccation tube.

4.2.2 Experimental validation of mouthpiece performance

In order to experimentally validate the simulation results, several mouthpieces were prepared by packing desiccant particles into cylindrical tubes. Different particle sizes of the desiccant were obtained by refining anhydrous calcium chloride pellets (Fisher Scientific, 4-20 mesh). These refined particles were size selected by sieving through wire meshes of predefined sizes. Average particle sizes of 1.15 mm and 0.65 mm were chosen for use. Cylindrical plastic mouthpiece (VacuMed, Part# 1018-22) with internal diameter of 22mm was used for packing these particles at porosity values of 0.425 and 0.365 respectively. Mouthpieces with three different lengths (12 mm, 24 mm, and 46 mm) were tested.

Humidity levels of the breath sample before and after passing through the mouthpiece were measured using a selected ion flow tube mass spectrometer (SIFT-MS) (Instrument science Ltd.) operating in multiple ion monitoring mode with H_3O^+ as the precursor ion [146]. The backpressure generated by the mouthpiece was measured using a pressure sensor (Freescale, Part# MP3V5004G) at a fixed sample flow rate. Sample flow rate from pressurized gas container (Praxair, Breathing grade air) was controlled with pressure regulators and monitored with a mass flow meter (Sensirion, EM1).

4.2.3 Integration of the mouthpiece with breath analyzers

The mouthpiece and a non-rebreathing T-valves (VacuMed, Part# 1464) were integrated into a portable breath nitric oxide sensor developed in our lab. The breath sensor was based on selective colorimetric change due to redox chemistry of phenylenediamine derivatives with the analyte [138]. Subjects blew directly into the mouthpiece for online measurement. The readings from the portable nitric oxide sensor were compared and correlated with chemiluminescence detection (Sievers NOA), which is the gold standard for nitric oxide measurement. Selective capture of humidity over some other gases by the desiccant material was tested with samples collected offline in metal laminated tedlar bags at a flow rate of 6.7 $L.min^{-1}$ using commercial sensors. Acetone and ammonia were measured with SIFT-MS, carbon dioxide was measured using absorption infrared based hand held monitor (Telaire® 7000 Series) and oxygen was measured using a portable electrochemical sensor (Vascular technologies).

4.3 Results and discussions

4.3.1 Simulation

Flow and mass transfer simulations were carried for several mouthpiece configurations. Figure 4.2(A) shows the flow profile obtained from a 30mm long desiccant tube, 15mm in diameter, packed with calcium chloride particles of 1.15 mm average diameter with a porosity of 0.425. For this porosity and particle size at a flow rate of 6.67 L.min^{-1}, the velocity field is homogenous due to porous properties of the structure, which is in contrast to parabolic velocity fields generally obtained under similar conditions in a non-porous free channel. Figure 4.2(B) shows the simulated pressure profile along the tube. The pressure drop increases with the increasing length of the packing material at a given packing density. Values for back pressure resulting from different particle sizes and porosities of packing for a given amount (5 g) of calcium chloride were also calculated as shown in Table 4.1.

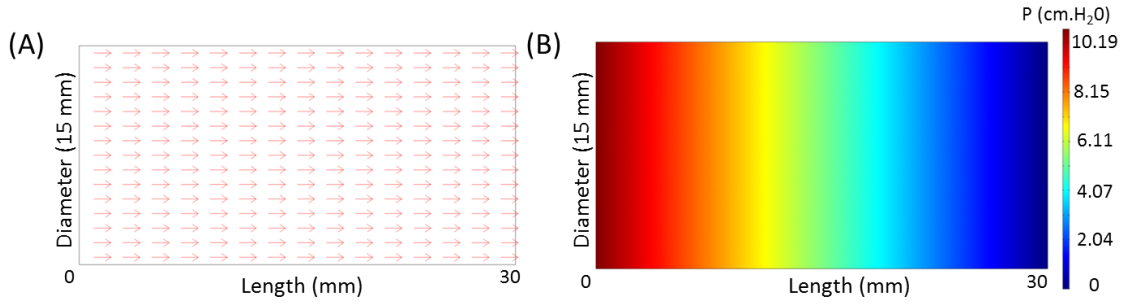

Figure 4.2: (A) Simulated velocity field along the tube shows uniform flow field established at a given flow rate of 6.67 L.min^{-1}, particle size of 1.15 mm and porosity of 0.425. (B) Simulated pressure profile along the tube showing increasing back pressure with tube length assuming uniform packing density.

Table 4.1: Simulated values of back pressure in cm H_2O generated in the desiccant mouthpiece for varying porosities and particle sizes. Simulation is for 5 grams of calcium chloride.

Particle size	Porosity				
	0.25	0.35	0.45	0.55	0.65
0.35 mm	243.50	66.68	22.46	8.23	3.01
0.70 mm	60.91	16.67	5.61	2.05	0.75
1.05 mm	27.07	7.41	2.49	0.91	0.33
1.40 mm	15.22	4.17	1.40	0.52	0.18

The data from table 1 provides guideline on packing of the desiccant material to achieve the desired back pressure range by changing either or both the particle size and the porosity of the mouthpiece. It is evident that back pressure at a given flow rate can be reduced by either increasing the particle size or the porosity of packing for a given mass of desiccant and mouthpiece geometry. Simulations were also carried out to obtain the effect of mouthpiece geometry (diameter and length) for a fixed particle size and porosity of packing assuming uniform packing density. Figure 4.3 plots pressure drop as a function of tube geometry with particles 1.15 mm in diameter packed with a porosity of 0.425. It is evident from the plot that the pressure drop decreases with increasing diameter and decreasing length of the mouthpiece for a given volumetric sample flow rate.

While providing an appropriate backpressure with the mouthpiece is an important requirement for many breath analyzers, other important parameters include the

desiccation efficiency, which should be considered together with the backpressure. For this reason the desiccation process was simulated. The desiccation of the breath along the tube (15 mm diameter, 30 mm length, 5 g calcium chloride, 1.15 mm particle diameter, porosity 0.425) is shown in Figure 4.4. Humidity of the sample decreases along the tube resulting in dryer output of the sample. Humidity levels at boundary 1 (inlet) and boundary 4 (outlet) were integrated for 30s in order to calculate of the efficiency (output/input %) of the desiccation process.

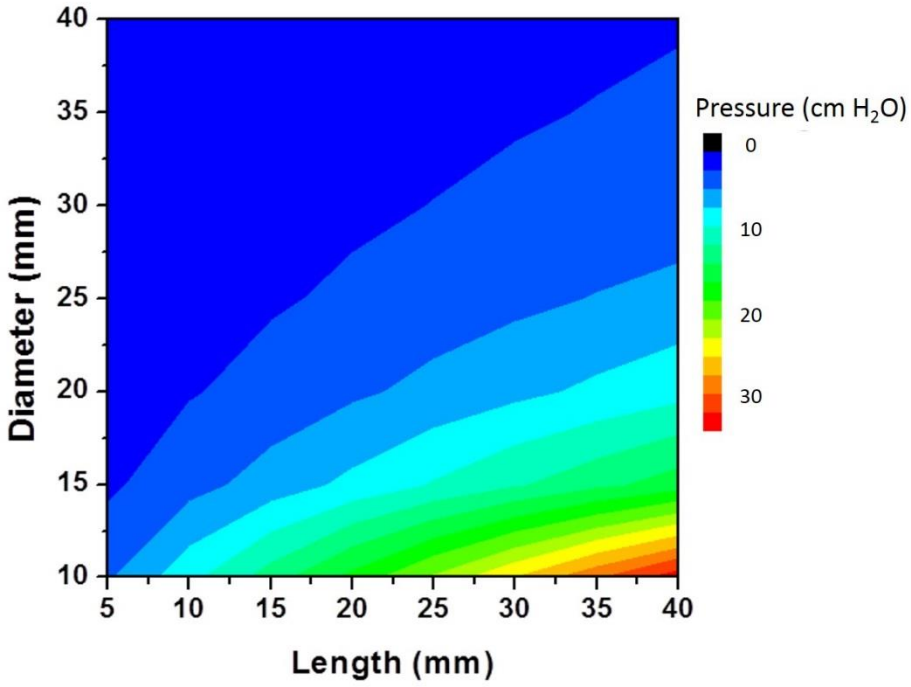

Figure 4.3: Pressure drop as a function of tube geometry for a given volumetric flow rate (6.67 $L.min^{-1}$).

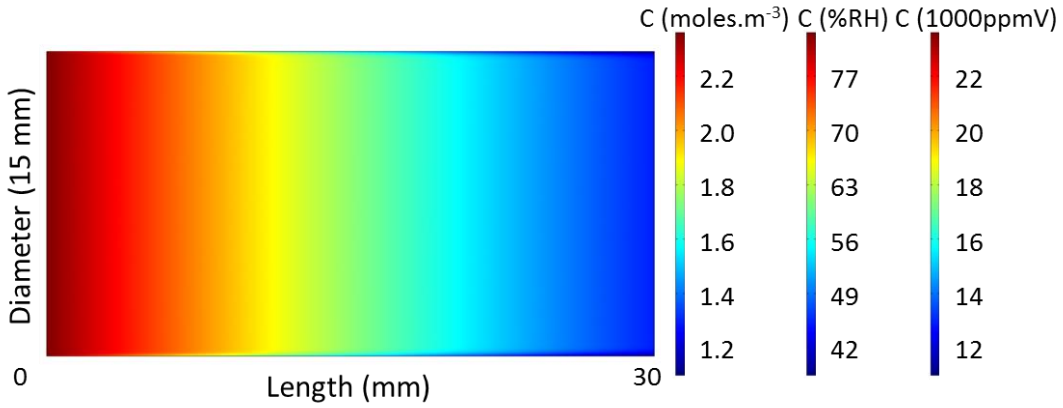

Figure 4.4: Simulation result of breath humidity concentration along the desiccation tube. Result is for a volumetric flow rate of 6.67 $L.min^{-1}$ and sampling time of 30 s through a desiccant tube (15 mm diameter, 30 mm length, 5 g calcium chloride, 1.15 mm particle diameter, porosity 0.425).

Desiccation efficiencies with different particle sizes of the desiccant particles were simulated for a given flow and amount of desiccant. Figure 4.5 shows the desiccation efficiency decreasing with increasing particle size for 5 g of calcium chloride. The efficiency was found to be independent of the packing porosity under these conditions. Desiccation efficiencies were also simulated for a fixed particle size and packing porosity with changing mouthpiece geometry (length and diameter). Figure 4.6 shows a plot of desiccation efficiency as a function of mouthpiece geometry with 1.15 mm wide particles packed with a porosity of 0.425. It can be seen from the plot that the efficiency of desiccation improves with increasing length and diameter (i.e., volume) of the mouthpiece.

These simulation results are useful in choosing the best parameters for preparing a customized mouthpiece for any breath analyzers. These parameters include mouthpiece

geometry (length and diameter), particle size and packing porosity. It is also clear that if any of these parameters are constrained based on particular needs of certain device then other parameters can be varied to achieve the desired performance.

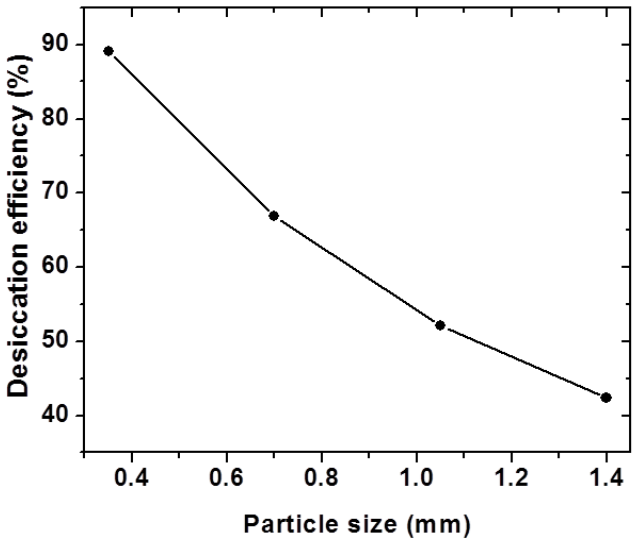

Figure 4.5: Desiccation efficiency for different particle sizes at a fixed geometry of the mouthpiece (15 mm long, 22 mm diameter) using 5 g of calcium chloride.

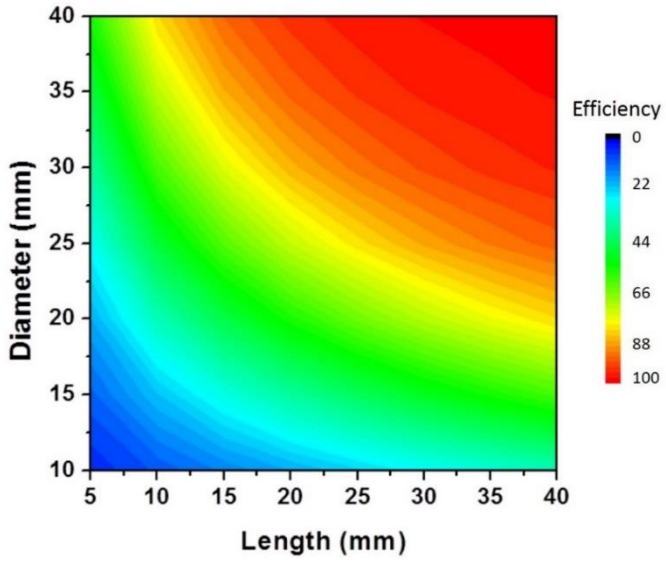

Figure 4.6: Desiccation efficiency simulated as function of tube geometry for volumetric flow rate of 6.7 $L.min^{-1}$.

4.3.2 Experimental validation of mouthpiece performance:

In order to validate the flow simulation, mouthpieces with three different lengths and 22 mm diameter were prepared. This geometry was chosen for easy integration with our device. Figure 4.7 shows the comparison of simulated to measured pressure difference across the tube for the three chosen lengths. Both results correlate well showing that the pressure drop increases with increasing length of the mouthpiece.

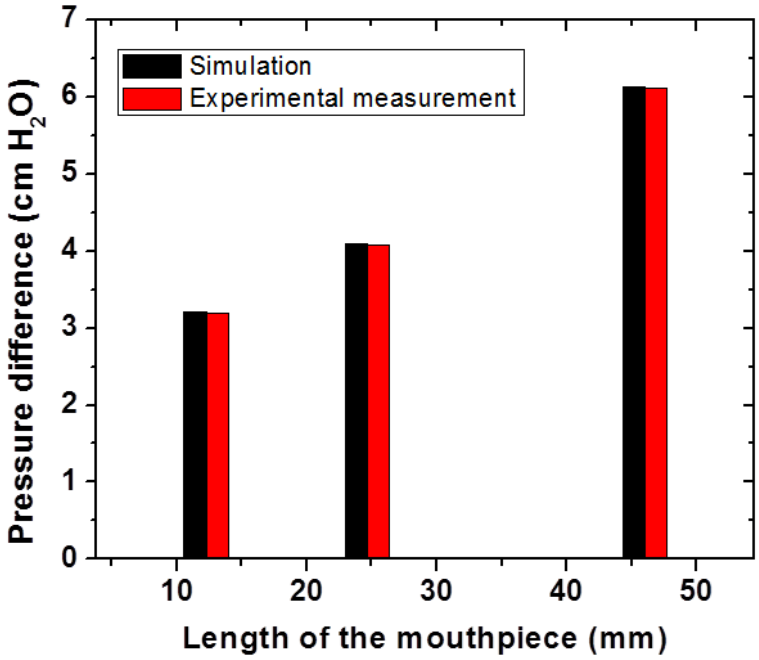

Figure 4.7: Comparison of simulated and experimentally measured pressure difference across the mouthpiece packed with 1.15 mm particles with a porosity of 0.425.

Table 4.2 shows a comparison of simulated and measured desiccation efficiencies for different mouthpiece geometries, packing and particle sizes. Deviations in the results increase at high desiccation efficiencies. With increasing desiccation, the experimental

efficiency is lower than the predicted efficiency from the model. This could be attributed to the exothermic nature of the desiccation process which starts to affect the efficiency for high humidity capture. Due to higher surface temperature the actual efficiency of capture is lower as observed in the experimental results.

Table 4.2: Comparison of simulated and measured desiccation efficiencies with different parameters of mouthpiece construction.

Length (mm)	Diameter (mm)	Particle size (mm)	Porosity	Simulated efficiency	Measured efficiency	Difference in Efficiency
12	22	1.15	0.425	44.1 %	43.6 %	0.5 %
25	22	1.15	0.425	68.8 %	66.49 %	2.31 %
49	22	1.15	0.425	89.3 %	81.54 %	7.76%
12	22	0.65	0.365	58.5 %	61 %	2.5%
15	22	0.65	0.365	69.6 %	68.4 %	1.2 %

Figure 4.8 shows humidity output of the mouthpiece over ten successive breathings measured by SIFT-MS. Each exhalation was followed by purging with dry air sample. It can be observed that the output was much drier initially and the efficiency of

the mouthpiece decreased with successive breathing cycles due to exhaustion and heating although the average humidity remained within the desired non condensing levels.

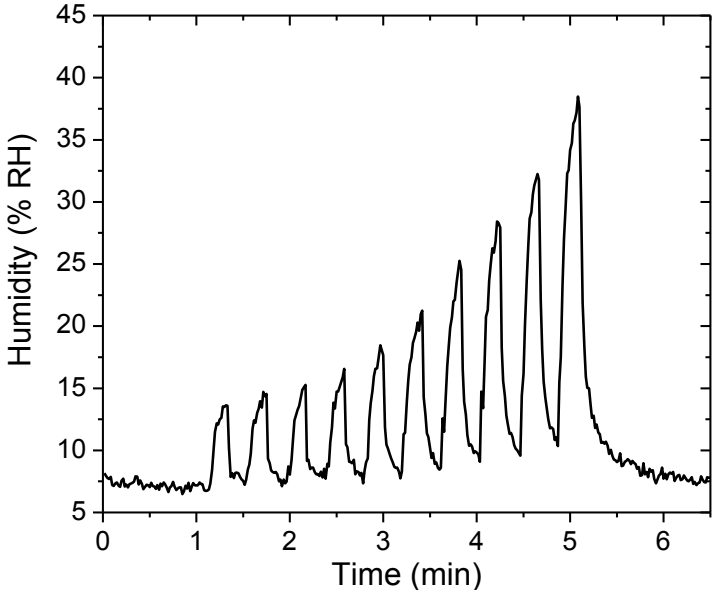

Figure 4.8: Humidity output of the mouthpiece (15 mm diameter, 30 mm length, 5 g calcium chloride, 1.15 mm particle diameter, porosity 0.425) for ten successive breathings. The baseline was obtained with dry air purging.

4.3.3 Integration with portable breath sensors

Desiccant mouthpiece with an efficiency of 70% (30 s sampling at 6.67 ml.min^{-1}) was used to sample breath in colorimetric optical sensor developed in our lab. Figure 4.9 (A) shows the response of the sensor to breath sampling without the mouthpiece. A jump in the intensity of signal can be observed in the sensing photodiode due to humidity condensation on the substrate affecting the transmittance [164]. Also, the reference photodiode shows random fluctuations in the signal. Response of the same sensor after integration of the mouthpiece is shown in Figure 4.9 (B). A linear decrease in intensity due to color development is observed without any spike due to humidity on the sensing

photodiode. The reference photodiode also shows a stable signal and fluctuations due to humidity are not observed. After integration of the mouthpiece, real breath samples could be analyzed for nitric oxide using the portable device as shown in Figure 4.10.

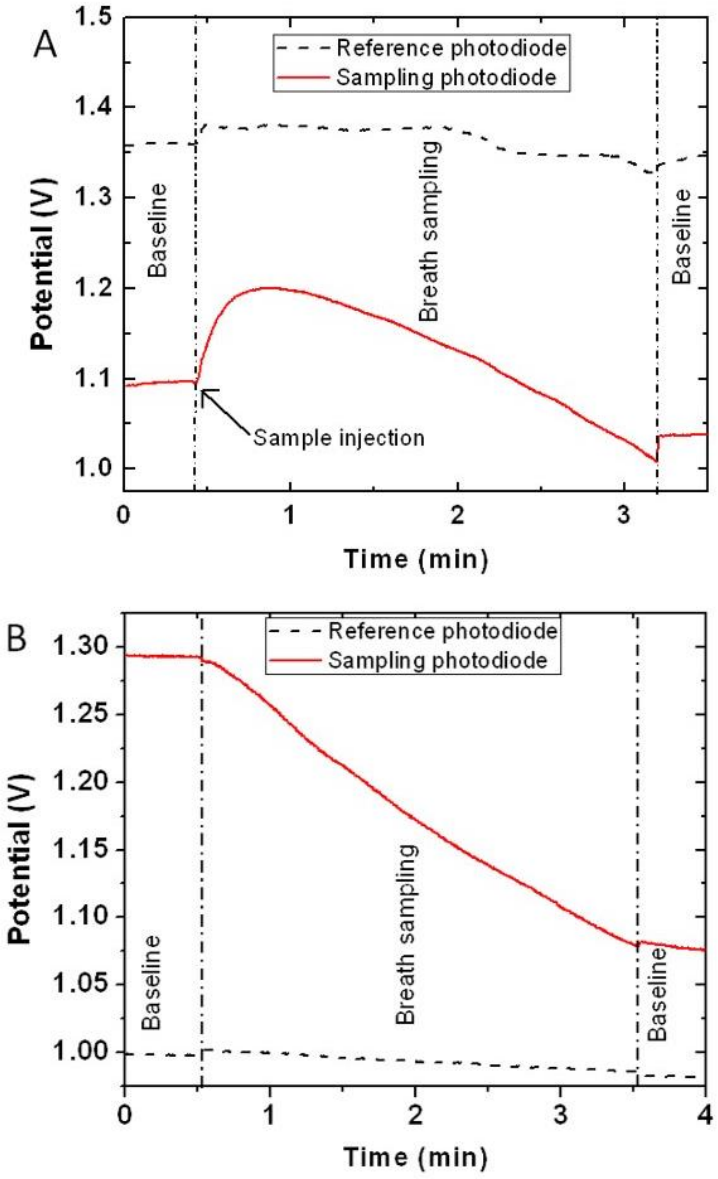

Figure 4.9: Optical response from photodiodes used for detection of color change (sampling) and correction (reference) in intensity during breath test (A) without the use of desiccant mouthpiece and (B) after integration of the desiccant mouthpiece.

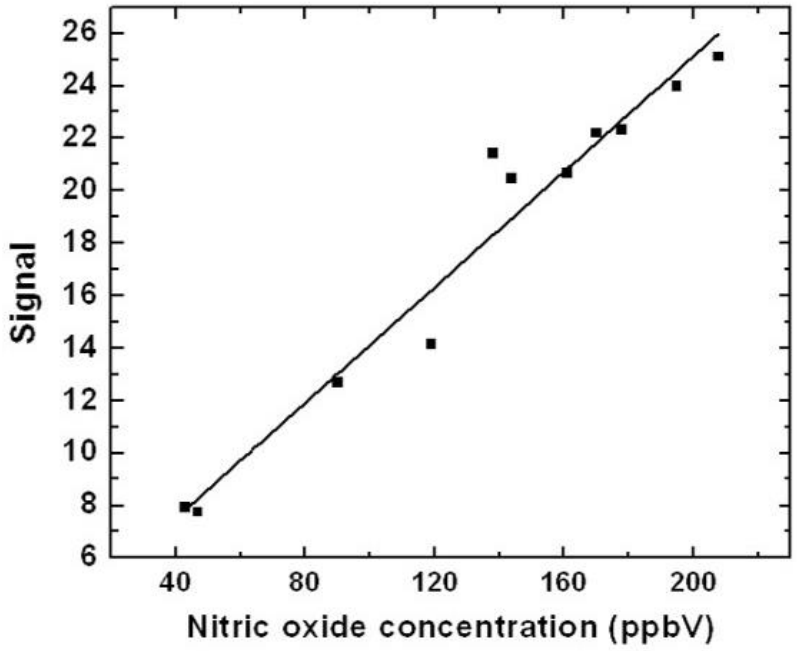

Figure 4.10: Analysis of nitric oxide levels in breath sample using colorimetric optical sensor integrated with the desiccation mouthpiece for online sample conditioning. A linear response is obtained towards nitric oxide.

4.3.4 Selectivity of the desiccation material:

The desiccation mouthpiece made of calcium chloride was tested for capture of some other gases including acetone, carbon dioxide, nitric oxide and oxygen for which the mouthpiece showed a capture efficiency of less than 5% for a 70% removal of humidity (Figure 4.11). These results show that the desiccant material can be used for analysis of these gases in conditioned breath by suitable sensors. However, there are some gases which can be captured by calcium chloride along with humidity. Ammonia is known to form complex with calcium chloride [165]. 10 ppmV input ammonia reduced to

0.8 ppmV output resulting in 92% ammonia removal efficiency of the calcium chloride mouthpiece under similar configuration.

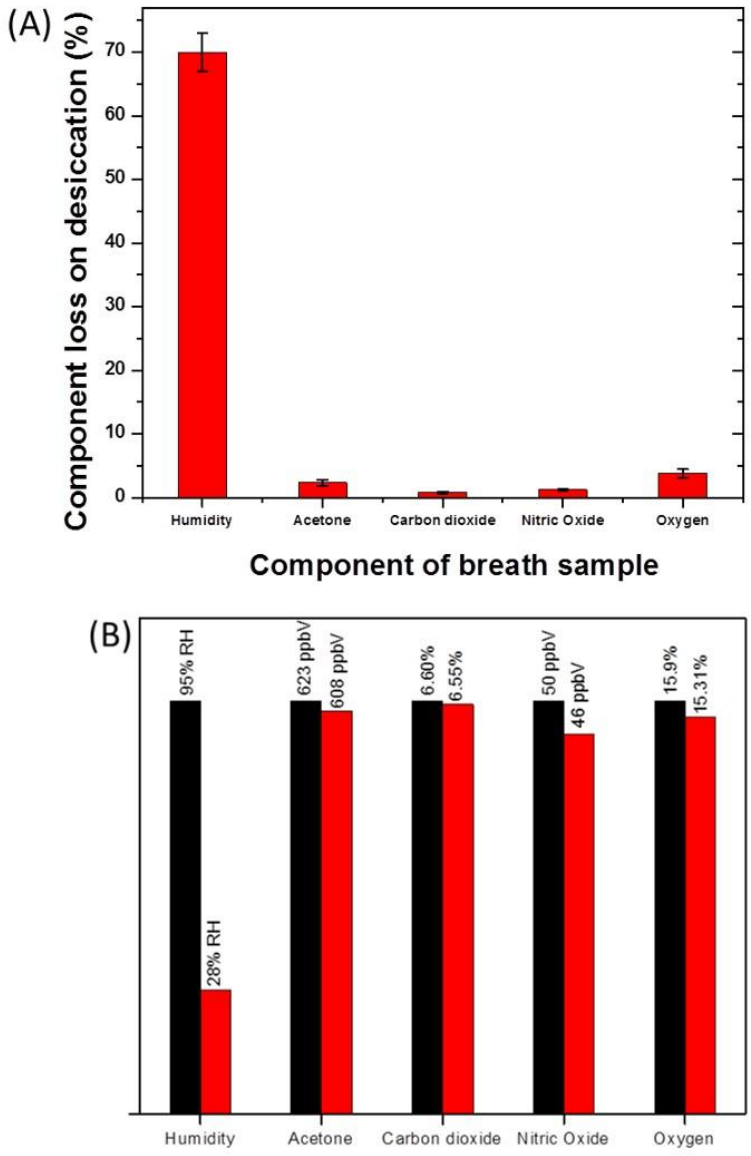

Figure 4.11: (A) Selective removal of humidity by the desiccant mouthpiece over other components of interest. (B) Absolute value of concentrations for different compounds tested before and after passing through the mouthpiece.

4.3.5 Reusability of the mouthpiece:

Reusability of the mouthpiece was tested for conditioning of real samples. Figure 4.12 (A) shows the efficiency of desiccation with variation of 5.6% at a mean efficiency level of 67.3% using a single mouthpiece for collection of ten samples with gap of 10mins between successive tests. Each sample was collected at a flow rate of 6.7 $L.min^{-1}$ to fill a 4 L tedlar bag. A gap of 10 min was given between each collection which was necessary to avoid efficiency loss due to overheating of the tube. The desiccation tube was also used for routine testing over a week. A single mouthpiece was used for sample collection, two times a day separated by 6 to 8 hours for six consecutive days. Figure 4.12 (B) shows the desiccation efficiency of each test. The mean efficiency for the six day test was 67.17% with a variation of 3.4%. The mouthpiece was stored in a regular zip-lock bag after each test. The storage was necessary because calcium chloride being hygroscopic adsorbs water continuously from the atmosphere. The zip-lock bag insulated the mouthpiece from the environment and avoided excessive humidity capture, which slowed the exhaustion of the mouthpiece.

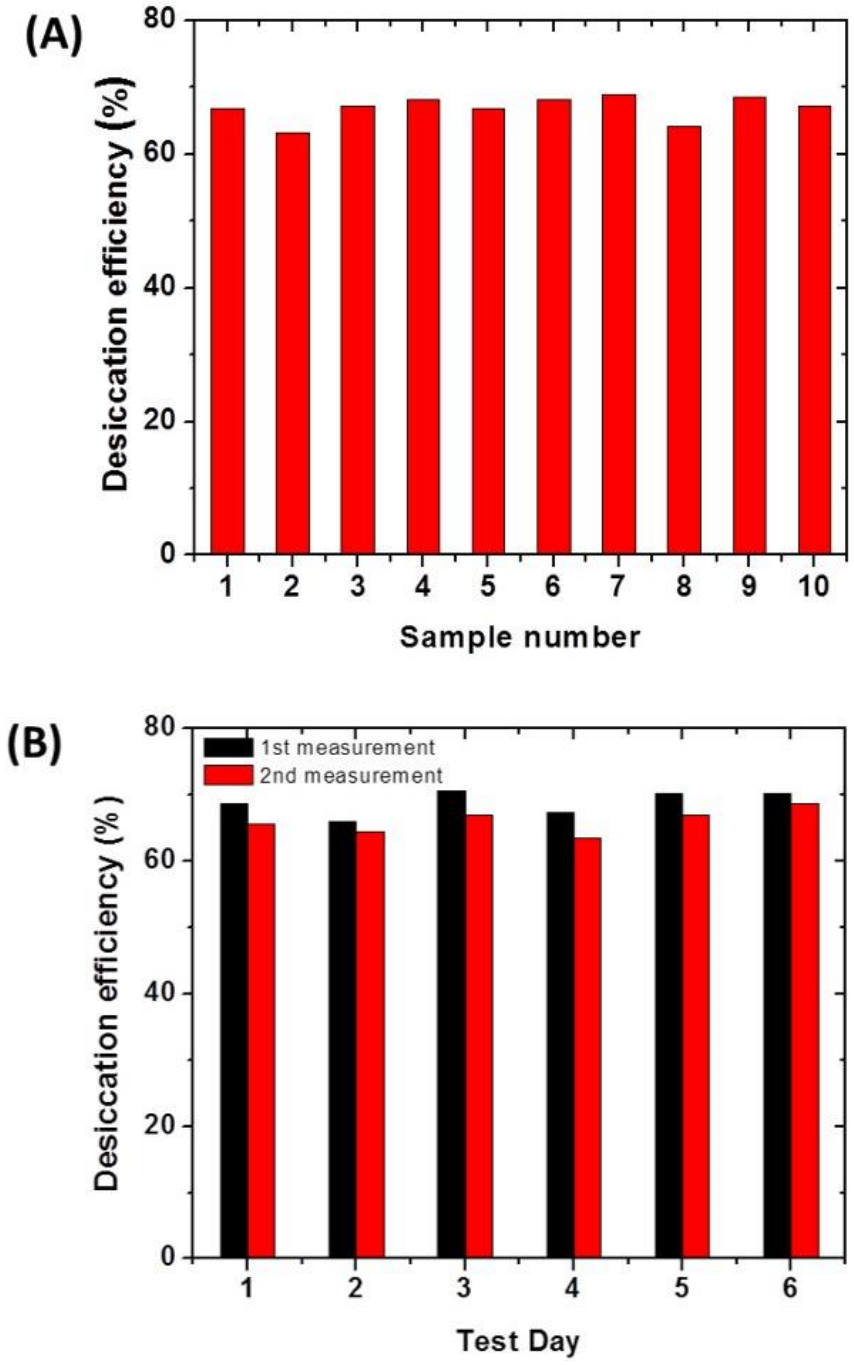

Figure 4.12: (A) Efficiency and reusability of one mouthpiece with 10 mins gap between successive tests. Mean desiccation efficiency (%) was 67.3 % and variation from the mean was 5.6 % (B) Reusability of one mouthpiece over a week measured two time each day and stored in plastic zip lock bag.

4.4 Conclusions

A miniaturized mouthpiece was developed to efficiently remove humidity and condition real breath samples in real time without affecting target analyte concentrations. The mouthpiece consists of packed desiccant particles in a tube. Numerical simulation of the desiccation process was carried out by taking into account various processes, including diffusion, mass transport and water absorption, described by differential equations with appropriate boundary conditions. The performance the mouthpiece in terms of humidity control and backpressure minimization depends on the size and packing density of the particles, geometry of the tube and flow rate. Based on the simulation, mouthpieces with different configurations were built and tested, and the experimental results validated the simulation findings. The findings provide guidance for those who wish to design efficient sample conditioning systems for practical chemical sensors, particularly breath analyzers. The mouthpiece was integrated into a handheld sensor for exhaled nitric oxide detection, and the results are in excellent agreement with gold standard methods. The miniaturized mouthpiece has great applicability for the new generation of portable breath analyzers, which require easy, efficient and reproducible removal of high humidity for seamless device functioning

5

SENSOR FOR DETECTION OF ACETONE IN EXHALED BREATH

5.1 Introduction

Acetone is one of the three ketone bodies found in our blood. These ketone bodies include acetoacetate (AcAc), which is generated during fatty acid metabolism in the liver, 3-β-hydroxybutyrate (3HB), which is formed by reduction of AcAc in the mitochondria and acetone, which is generated as a result of spontaneous decarboxylation of AcAc (Figure 5.1) [166, 167].

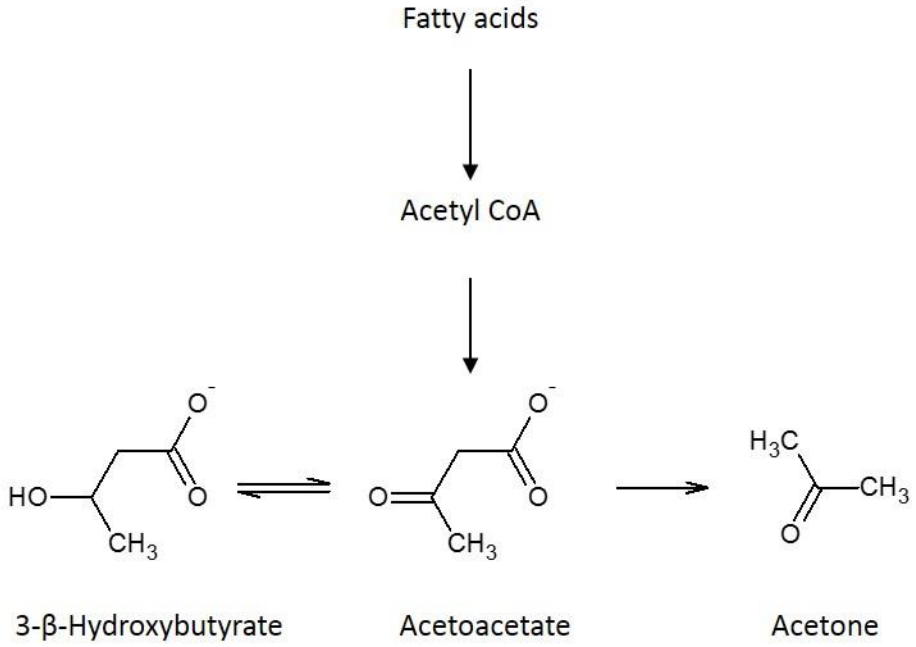

Figure 5.1: Ketone bodies in the blood

The process of production of ketone bodies is called ketogenesis which takes place in mitochondria of liver cells [168, 169]. The liver can produce up to about 185 g of

ketone bodies in healthy adults per day. The process starts with β-oxidation of fatty acids to acetyl CoA which is converted to acetoacetyl CoA catalyzed by 3-ketothiolase. Acetoacetyl CoA is then converted to 3-hydroxy-3-methylglutaryl CoA (HMG CoA) by mitochondrial HMG CoA synthase. This step is stimulated by starvation, low levels of insulin, and consumption of a fat rich diet [170]. HMG CoA is cleaved by HMG CoA lyase to release AcAc which is reduced to 3HB by 3-hydroxybutyrate dehydrogenase (HBD). This reduction is accompanied by oxidation of NADH to NAD^+. Thus, the ratio of 3HB to AcAc in the blood depends on the ratio of $NADH/NAD^+$ in the hepatic mitochondria. These ketone bodies serve as fuel when glucose is not readily available [171] and reduce proteolysis [172, 173]. Being short chain organic acids, ketone bodies can freely diffuse across cell membranes [174, 175]. For this reason, brain which cannot utilize fatty acids for energy is dependent on ketone bodies for energy in case of glucose depletion. Ketone bodies supply about 2/3 of the brain's energy needs during prolonged fasting and starvation [176]. A schematic of relationship of glucose and fatty acid metabolism leading to formation of ketone bodies in liver cells is shown in Figure 5.2. Acetyl CoA which is the common metabolite after glycolysis of glucose or β-oxidation of fatty acids condenses with oxaloacetate to enter the citric acid cycle. Oxaloacetate is derived from pyruvate during glycolysis by the action of pyruvate decarboxylase. Therefore, for acetyl CoA to enter the citric acid cycle a sufficient level of glycolysis is required. If body is depleted of glucose then oxaloacetate is preferentially utilized in glucose generation by gluconeogenesis, instead of condensing with acetyl CoA. Acetyl CoA is then diverted to ketone body formation.

Ketosis is the state characterized by elevated levels of ketone bodies in the body. Hyperketonemia which is elevated concentration of ketone bodies in the blood and ketoacidosis which results into decrease in blood pH due to excessive accumulation of ketone bodies in the blood can result from ketosis. Ketosis can be caused both by physiological and pathological processes.

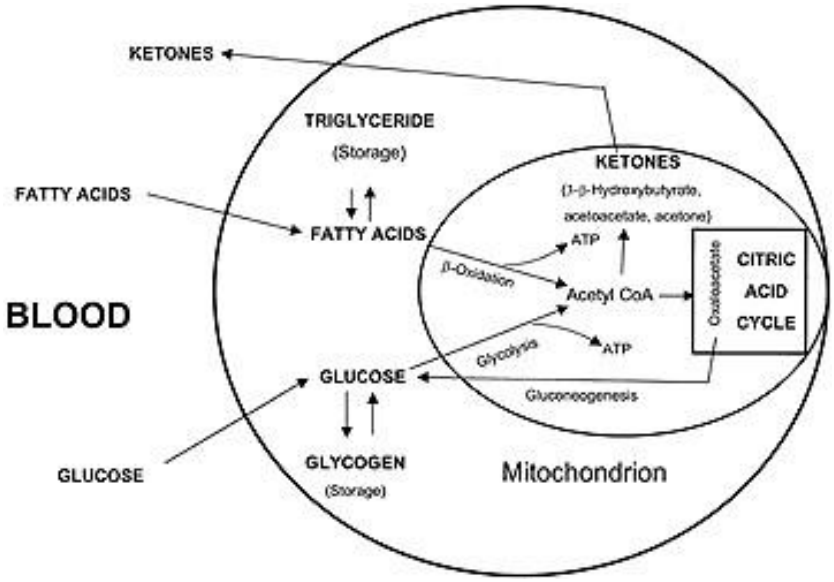

Figure 5.2: Ketone body production in hepatocytes [177].

Physiological processes which mainly result into hyperketonemia include fasting, prolonged exercise, or consumption of fat rich ketogenic diets. Fasting in adults may result into mild increase in ketone bodies. Ketone concentrations may rise above 1.0 mM after a fast of 3 days and reaching a plateau of 6-8 mM after 4 weeks of starvation. In newborn infants, ketosis may occur due to fasting resulting from non-availability of food. This could be caused by mild infections usually associated with vomiting and diarrhea [178]. Ketone levels in such conditions may rise up to 1 mM. Ketogenic diets commonly

used for weight loss programs [179, 180] treating epileptic children [181, 182] and prolonged exercise also result in physiological ketosis in which ketone body levels rise in the range of 1-2 mM [183, 184]. Pathological processes resulting in ketosis include diabetes mellitus, cortisol and growth hormone deficiency, toxic ingestions of ethanol or salicylates and certain rare inborn errors of metabolism. Of these, the most common causes of ketosis are diabetic ketoacidosis (DKA) and toxic ketoacidosis. DKA generally happens in type 1 diabetic patients but is also reported in type 2 diabetic patients [185, 186]. DKA is characterized by uncontrolled hyperglycemia, metabolic acidosis, and increased total body ketone concentrations. DKA is dangerous compared to ketosis in normal people because insulin deficiency combined with hormonal imbalance i.e. increased levels of counter regulatory hormones (catecholamine, cortisol, glucagon, and growth hormone) leads to release of free fatty acids into circulation and uncontrolled oxidation by liver cells [187, 188]. In normal people insulin serves as a check on uncontrolled ketosis. DKA is a life threatening complication of diabetes. It is responsible for more than 500,000 hospital days per year and an estimated direct and indirect medical expense of 2.4 billion USD in United States [189-192].

Measuring blood or urine ketone levels is recommended for monitoring ketosis due to both physiological reasons like ketogenic diet [193] and pathological reasons like DKA [194, 195]. Most commonly used methods for measuring ketone bodies include urine dipsticks and electrochemical capillary blood monitors. Urine dipsticks utilize the nitroprusside reaction producing purple color upon complex formation with AcAc. This gives a semi-quantitative measure of AcAc and to some extent measure acetone with the

use of glycine but does not indicate 3HB [196]. Monitoring 3HB levels is of importance because during DKA the ratio of 3HB to AcAc changes from 1:1 to about 10:1. So, monitoring AcAc alone does not indicate the overall ketosis state. Laboratory analysis of 3HB includes enzymatic assays which are time consuming and cannot be used for emergency diagnosis and management of DKA. Electrochemical sensors are available, for example Precision XtraTM (Abbott Diabetes Care, Inc. CA, USA), which measure electrical current proportional to 3HB concentrations in blood [197]. This method is currently approved and is used both at home and clinical settings [198].

Though, currently methods exist for monitoring ketosis they suffer from several drawbacks of being qualitative, slow in response to change in blood ketone or invasive. Breath acetone has been shown to be a reliable indicator of ketosis and it correlates with the levels of AcAc and 3HB in the blood [199, 200]. Studies have shown higher levels of breath acetone in diabetic patients compared to normal controls [59, 201]. Breath acetone has also been used for identification of diabetes [202]. A portable breath acetone sensor would not only help in non-invasive monitoring of ketosis which is valuable for managing DKA but it will also be useful for monitoring outcomes of diet regiments and exercise routines for weight management and epilepsy control. This chapter outlines efforts made towards development of such a platform utilizing colorimetric response of a pH indicator upon reaction of acetone with hydroxylamine acid salt. An overall approach of sensor development with sample conditioning and data analysis is presented.

5.2 Experimental

5.2.1 Detection setup

The detection setup similar to that developed for nitric oxide sensor based on optical detection of a colorimetric reaction was used. The setup used two photodiodes, one of the photodiodes captured light transmitted through chemically modified substrate which provided signal from the chemical change whereas the other photodiode captured light transmitted through the reference region devoid of chemical modification (Figure 5.3). Photodiode readings from both the sensing and the reference regions were used to calculate the change in absorbance.

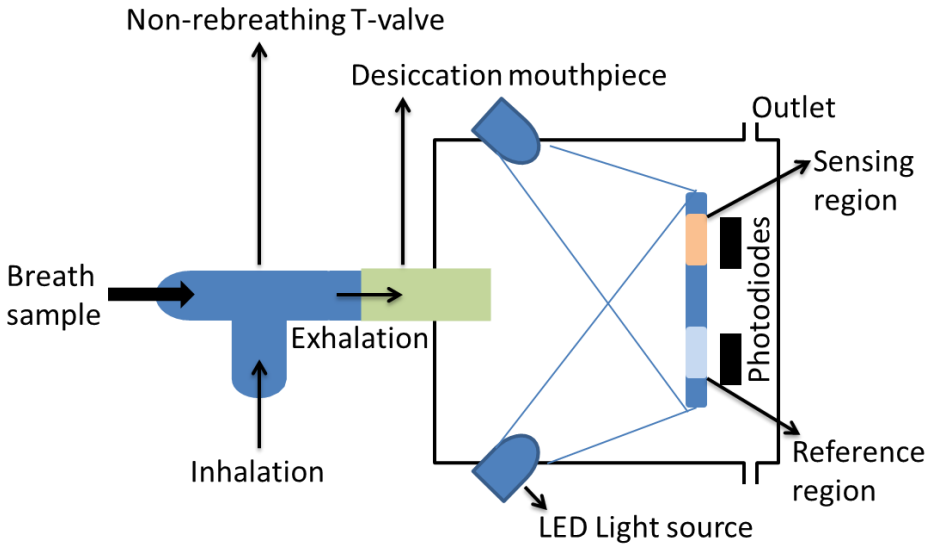

Figure 5.3: Schematic representation of acetone detection setup.

5.2.2 Artificial gas samples

Artificial gas samples were prepared by injecting 100 µl of acetone solution into a 4 L metal laminated tedlar bag filled with breathing grade air (Praxair, Inc.). Appropriate

volume of this high concentration acetone sample was injected in a bigger 40 L metal laminated tedlar bags filled with humidified air. Humidity and acetone concentrations were quantified in the bags using MIM mode of SIFT MS. The bigger bags were diluted or concentrated based on the quantification results to achieve the desired concentration.

5.2.3 Chemical reaction

The detection chemistry for acetone detection was based on pH change of based on Figure 5.4.

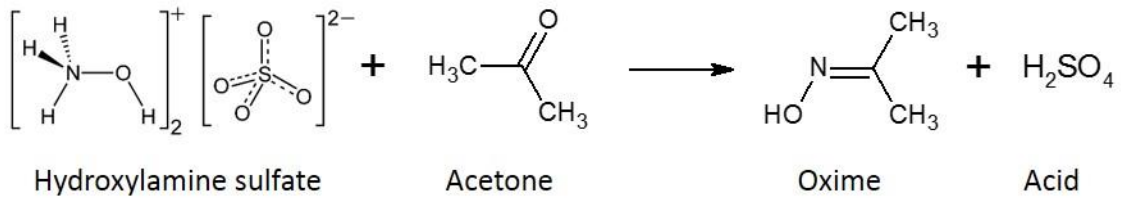

Figure 5.4: Acetone reaction with hydroxylamine acid salt.

The change in pH due to the released acid was measured by the colorimetric response of thymol blue 555 nm.

5.2.4 Sampling of breath

Offline collection of breath samples was done in 4 L metal laminated tedlar bags. The subject used a non-rebreathing T-valve (VacuMed, Part# 1464) to breathe into the bag without any flow regulation. For online breath samples, a desiccation tube was integrated with the non-rebreathing T-valve. The pressure difference was correlated with the flow rate measured with a digital mass flow meter (Sensirion, EM1). During breath

sampling the flow rate was integrated over time using an in house built microcircuit and processing software to indicate completion of 4 L of sampling.

5.3 Results and discussions

5.3.1 Sample regulation

Breath samples were collected in real time by allowing subjects to blow directly into the device. The volume of the sample delivered to the device was fixed at 4 L. This was done by measuring pressure difference along the sampling line. The pressure difference was correlated with the flow rate (Figure 5.5) in a range of 0.5 to 10 $L.min^{-1}$ within which most of the subjects would blow into the device. The correlation graph was implemented through hardware developed in CBB to indicate the user when the target sampling volume was reached. The mean value of 4 L was achieved with a 3% coefficient of variation as shown in Figure 5.6.

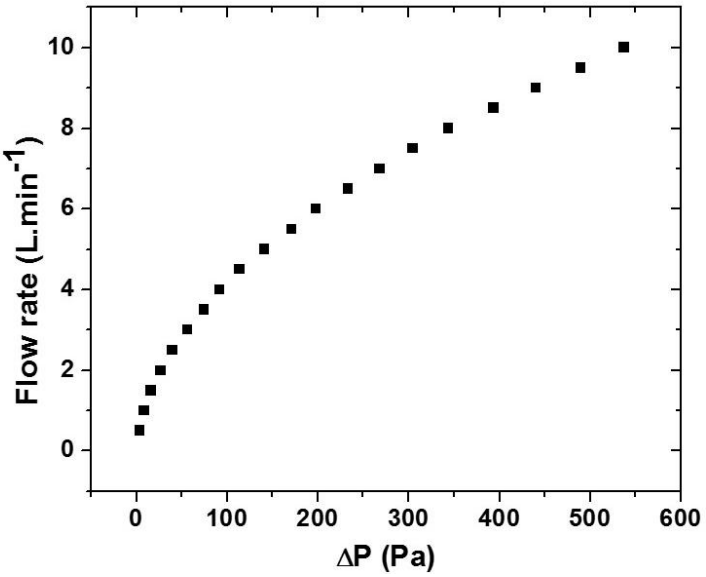

Figure 5.5: Relationship between the sample flow rate and the pressure difference along the sampling line. The relationship was used to reach a target volume by measuring the pressure difference while sampling.

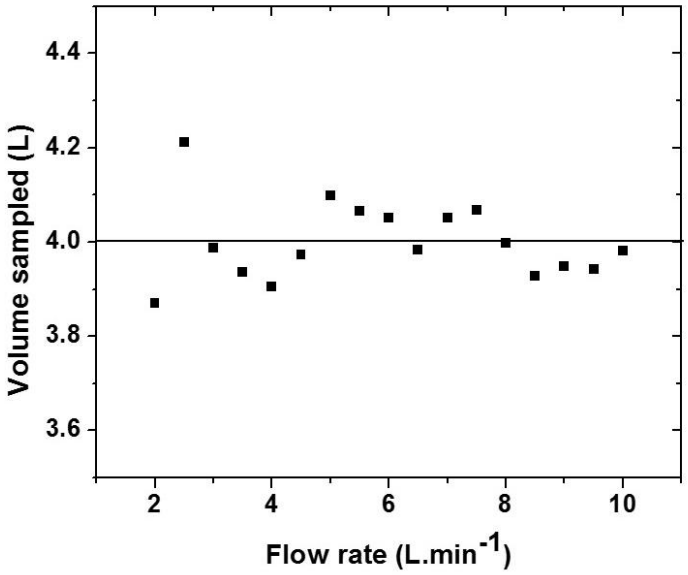

Figure 5.6: Volume sampled into the device at different sample flow rates. The mean sampled volume was 4 L and the coefficient of variation was 3%.

5.3.2 Sensor calibration

Response of the sensor towards acetone was measured in a range from 0.5 ppmV to 100 ppmV. This wide range of concentrations was chosen to reflect a broad range of breath acetone levels expected for normal subjects as well as diabetics and individuals under ketogenic diets [58, 203, 204]. As shown in Figure 5.7(A), the response to acetone was linear in lower concentration range up to 20 ppmV. Figure 5.7(B) shows the response of the acetone sensor at higher concentrations, which followed a non-linear Langmuir-like behavior. Langmuir equation was used to fit the sensor response, with a resulting squared-correlation coefficient (R^2) of 0.995. It is worth noticing that five tests were performed at each concentration, and relatively reproducible results were obtained (error bars represent standard deviation from 5 tests).

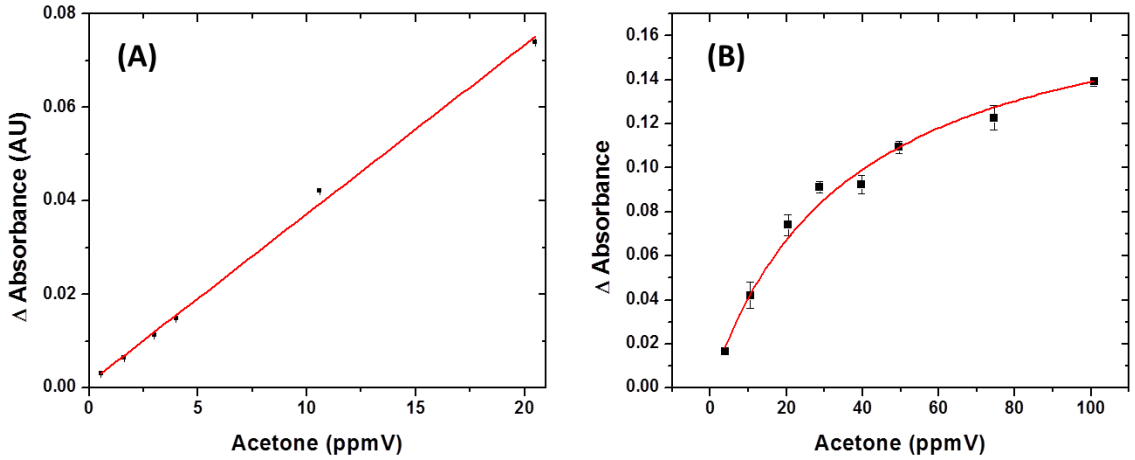

Figure 5.7: Sensor calibration: (A) Linear response observed for acetone concentration up to 20 ppmV. Calibration slope = 0.00362± 0.00009 ΔAbsorbance (AU) / Acetone (ppmV) (intercept = 0) with a correlation coefficient of 0.997. (B) Overall response up to

100ppmV fitted on Langmuir equation curve ΔAbsorbance (AU) = 0.19X/(36.57 + Acetone (ppmV)) with a correlation coefficient of 0.995.

5.3.3 Correlation with SIFT-MS

The sensor was used to measure acetone concentration in breath of three fasting subjects and the data was correlated with measurements from SIFT-MS. Figure 5.8 shows the correlation plot of the data obtained with a correlation coefficient of 0.96 and slope of 1. The data was normalized by the total exhalation time taken to reach the target sample volume.

The limit of agreement between the acetone sensor and SIFT-MS was determined from Bland-Altman plot as shown in Figure 5.9. The difference between the readings from acetone sensor and corresponding reading from SIFT-MS was plotted against the average reading from SIFT-MS and the acetone sensor. The limit of agreement was ±1.96 standard deviations from the mean which was within 1 ppmV. This means that within 95% confidence the reading from the sensor is within 1 ppmV difference from the reading obtained from SIFT-MS.

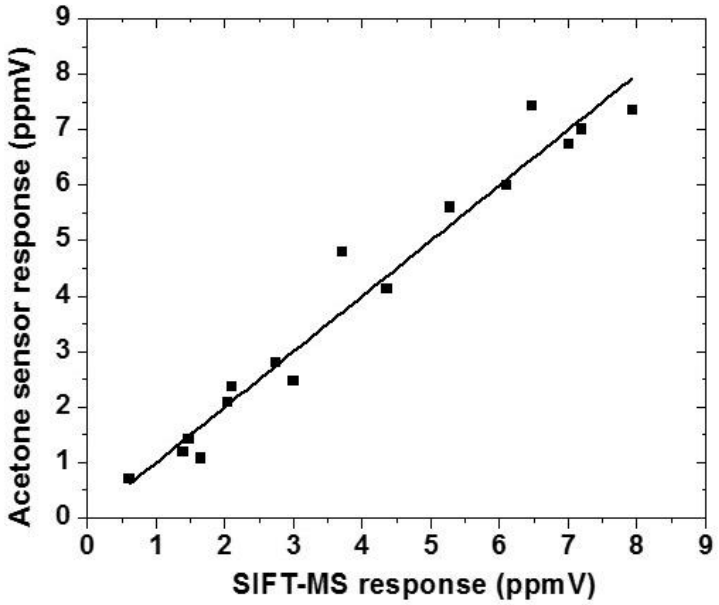

Figure 5.8: Correlation of the acetone sensor with SIFT-MS. Coefficient of correlation was 0.96 and slope was 1.

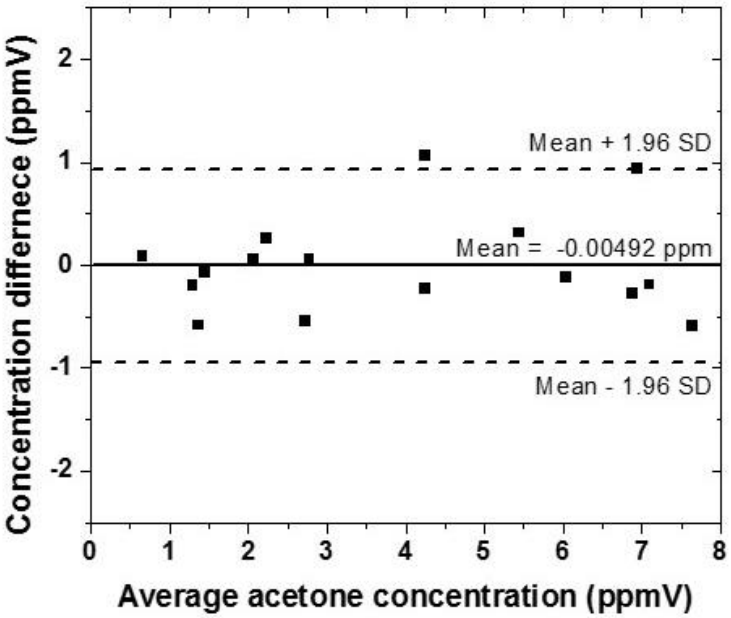

Figure 5.9: Bland-Altman plot showing limit of agreement between acetone sensor and SIFT-MS to be within 1 ppmV.

5.3.4 Reproducibility of sensors

Sensor responses were tested for variability both in intra and inter batch preparation. Figure 5.10 shows response of 60 sensors towards 4 ppmV acetone prepared in eight different batch. Coefficient of variation within a single batch was less than 15%. Overall mean of the normalized signal obtained for 60 sensors tested was 0.0129 with a 17% coefficient of variation.

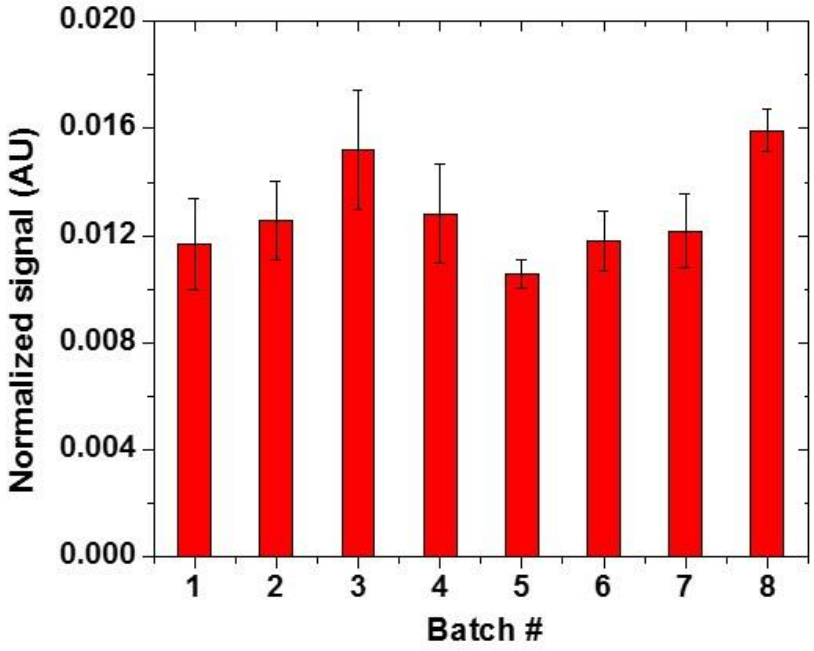

Figure 5.10: Normalized signal towards 4 ppmV acetone of 60 sensors prepared in 8 different batches.

5.3.5 Monitoring Ketosis

In order to test the capability of the sensor device for monitoring breath acetone release associated to ketone levels, two subjects were tested. Subject 1 was measured while the

ketone levels were building up during fasting. As shown in Figure 5.11(A), Subject 1 had a breath acetone level of 2.4 ppmV in the morning and reached a value of 6.6 ppmV after 8 hours of fasting during the day. This trend was expected according to previous clinical studies under similar conditions [55]. On the other hand Subject 2, prior to testing, had developed ketosis induced by fat rich ketogenic diet. Subject 2 had a high breath acetone concentration of 8 ppmV in the morning. Subject's breath acetone levels were followed after intake of a carbohydrate rich meal. The breath acetone level of the subject decreased from 8ppmV to about 2 ppmV after 8 hours (Figure 5.11(B)) as expected due to clearance of ketones induced by replacement of lipolysis by glycolysis. These tests clearly demonstrated the utility of the developed sensor in monitoring ketone buildup and clearance. This would be useful both in monitoring the development of state of ketosis or onset of ketoacidosis and its effective treatment.

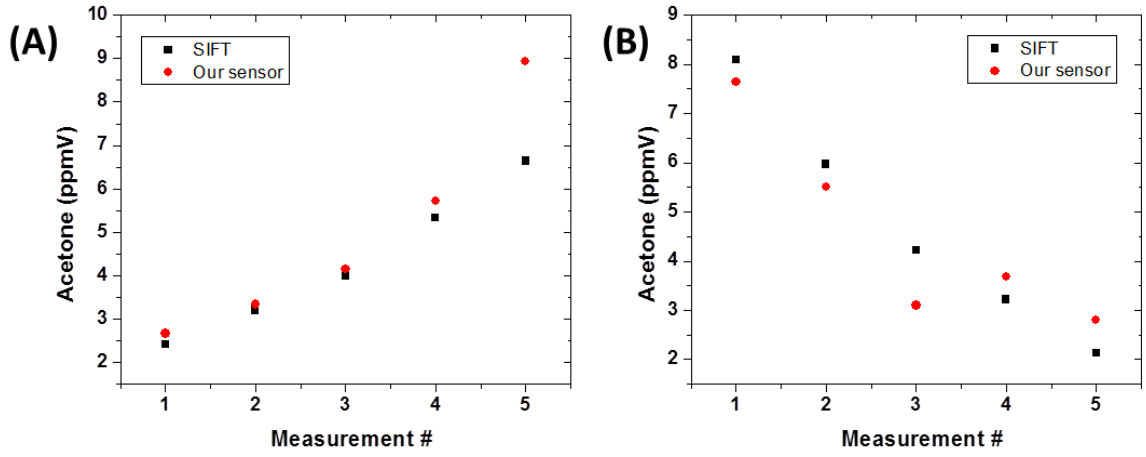

Figure 5.11: Breath acetone levels assessed in individuals under fasting/diet-induced ketosis. (A) Monitoring breath acetone of Subject 1 building ketones during the fasting

period. (B) Monitoring breath acetone of Subject 2 during ketone clearance after intake of carbohydrate rich diet after ketogenic diet intake.

5.4 Conclusions

In conclusion, a colorimetric sensor for acetone measurement in exhaled human breath has been developed. Strategies to overcome confounding effect of humidity interference have been implemented. Analysis of real breath samples with subjects directly blowing into the sensor without the use of a pump for sample collection has been shown. The developed sensor has reproducible and stable response to be useful for monitoring the state of ketosis and ketoacidosis.

6

CONCLUSIONS AND FUTURE DIRECTIONS

The work presented in this thesis has demonstrated the development of portable sensors for detection of specific breath analytes. Nitric oxide and acetone were chosen for detection because of their importance in monitoring health and fitness status of the body. Nitric oxide correlates with lung inflation and acetone reflects the level of ketosis in the body. Colorimetric detection was chosen for the reason of simplicity and cost effective implementation. Specific colorimetric reactions suitable for detection of each analyte were chosen and optimized for sensitive detection. Platforms for optical detection of the color change were developed in a simple and cost effective setup. Issues in the sampling procedures were identified and a solution to condition the breath samples was developed. The variability in sampling and its effect on detection was discussed and addressed. The developed sensor's applications were demonstrated by analyzing real breath samples from subjects directly blowing into the sensors.

This work can be extended in multiple directions. The developed sensor devices can be used to perform epidemiological studies. Portability, ease of use and mobile compatibility of the devices for data communication and processing make them ideal for conducting such studies in free living conditions which is difficult otherwise. Another future work from device point of view could be to integrate multiple analyte detection into one device. Since both nitric oxide and acetone sensors utilize optical detection, they could share the same hardware. Though, there are several challenges which include different sampling and detection requirements, in principle this can be achieved.

Otherwise, chemistries can be developed to detect other analytes of importance in the breath which can use the developed optical detection platform. For example, ammonia for monitoring renal diseases and sulfides for monitoring liver health could be explored. The developed sensors could be integrated with other physical sensors to monitor physiological parameters such as heart rate, or body fat. These sensors can also be integrated with appropriate sampling techniques and optimized for environmental monitoring at a personal level.

Given the immense potential of breath sensing in disease diagnosis, monitoring and management I believe that such portable sensors will attract more attention in the future. More and more such sensors will come out of the lab space and be available as affordable products to serve the needs of the society.

REFERENCES

1. Smith, D. and P. Spanel, *The novel selected-ion flow tube approach to trace gas analysis of air and breath.* Rapid communications in mass spectrometry, 1999. **10**(10): p. 1183-1198.

2. Španěl, P. and D. Smith, *Progress in SIFT-MS: Breath analysis and other applications.* Mass Spectrometry Reviews, 2010. **30**(2): p. 236-267.

3. Phillips, M., et al., *Variation in volatile organic compounds in the breath of normal humans.* Journal of Chromatography B: Biomedical Sciences and Applications, 1999. **729**(1): p. 75-88.

4. Miekisch, W., J.K. Schubert, and G. Noeldge-Schomburg, *Diagnostic potential of breath analysis--focus on volatile organic compounds.* Clinica chimica acta; international journal of clinical chemistry, 2004. **347**(1-2): p. 25.

5. Klein, P., et al., *Noninvasive detection of Helicobacter pylori infection in clinical practice: the 13C urea breath test.* The American journal of gastroenterology, 1996. **91**(4): p. 690.

6. Cone, E.J., *Oral fluid testing: new technology enables drug testing without embarrassment.* CDA. JOURNAL, 2006. **34**(4).

7. Schwarz, K.B., et al., *Possible antioxidant effect of vitamin A supplementation in premature infants.* Journal of pediatric gastroenterology and nutrition, 1997. **25**(4): p. 408-414.

8. Refat, M., et al., *Utility of breath ethane as a noninvasive biomarker of vitamin E status in children.* Pediatric research, 1991. **30**(5): p. 396-403.

9. Schubert, J.K., et al., *Breath analysis in critically ill patients: potential and limitations.* Expert Review of Molecular Diagnostics, 2004. **4**(5): p. 619-629.

10. Tisch, U., et al., *Detection of Alzheimer's and Parkinson's disease from exhaled breath using nanomaterial-based sensors.* Nanomedicine, 2012(xx): p. 1-14.

11. Probert, C., et al., *Volatile organic compounds as diagnostic biomarkers in gastrointestinal and liver diseases.* J Gastrointestin Liver Dis, 2009. **18**(3): p. 337-343.

12. Turner, C., *Potential of breath and skin analysis for monitoring blood glucose concentration in diabetes.* Expert Review of Molecular Diagnostics, 2011. **11**(5): p. 497-503.

13. Ongole, R. and N. Shenoy, *Halitosis: Much beyond oral malodor.* Kathmandu University Medical Journal, 2010. **8**(2): p. 269-275.

14. Pauling, L., et al., *Quantitative Analysis of Urine Vapor and Breath by Gas-Liquid Partition Chromatography.* Proceedings of the National Academy of Sciences, 1971. **68**(10): p. 2374-2376.

15. Jansson, B. and B. Larsson, *Analysis of organic compounds in human breath by gas chromatography-mass spectrometry.* The Journal of laboratory and clinical medicine, 1969. **74**(6): p. 961.

16. Chen, S., V. Mahadevan, and L. Zieve, *Volatile fatty acids in the breath of patients with cirrhosis of the liver.* The Journal of laboratory and clinical medicine, 1970. **75**(4): p. 622.

17. Riely, C.A., G. Cohen, and M. Lieberman, *Ethane Evolution: A New Index of Lipid Peroxidation.* Science, 1974. **183**(4121): p. 208-210.

18. Dannecker Jr, J.R., E.G. Shaskan, and M. Phillips, *A new highly sensitive assay for breath acetaldehyde: Detection of endogenous levels in humans.* Analytical Biochemistry, 1981. **114**(1): p. 1-7.

19. Davis, C., et al., *Editorial The Future of Sensors and Instrumentation for Human Breath Analysis.* Sensors Journal, IEEE, 2010. **10**(1): p. 3-6.

20. Cikach, F.S. and R.A. Dweik, *Cardiovascular Biomarkers in Exhaled Breath.* Progress in Cardiovascular Diseases, 2012. **55**(1): p. 34-43.

21. Minh, T.D.C., D.R. Blake, and P.R. Galassetti, *The clinical potential of exhaled breath analysis for diabetes mellitus.* Diabetes Research and Clinical Practice, 2012.

22. Davies, S., P. Spanel, and D. Smith, *Quantitative analysis of ammonia on the breath of patients in end-stage renal failure.* Kidney international, 1997. **52**(1): p. 223.

23. Lewicki, R., et al. *Real time ammonia detection in exhaled human breath using a distributed feedback quantum cascade laser based sensor*. in *Proc. of SPIE Vol*. 2011.

24. Risby, T.H. and S.S. Sehnert, *Clinical application of breath biomarkers of oxidative stress status.* Free Radical Biology and Medicine, 1999. **27**(11): p. 1182-1192.

25. Kohlmüller, D. and W. Kochen, *Is n-pentane really an index of lipid peroxidation in humans and animals? A methodological reevaluation.* Analytical Biochemistry, 1993. **210**(2): p. 268.

26. Istepanian, R., S. Laxminarayan, and C.S. Pattichis, *M-health: emerging mobile health systems.* M-Health: Emerging Mobile Health Systems, Edited by R. Istepanian, S. Laxminarayan, and CS Pattichis. 2006 XXX, 624 p. 182 illus. 0-387-26558-9. Berlin: Springer, 2006., 2006. **1**.

27. TORGAN, C. *The mHealth Summit: Local & Global Converge*. 2009 [cited 2013 July]; Available from: http://www.caroltorgan.com/mhealth-summit/.

28. Organization, W.H., *World health statistics 2012*2012: World Health Organization.

29. Union, I.T. *ICT Facts and figures*. 2013; Available from: http://www.itu.int/en/ITU-D/Statistics/Pages/facts/default.aspx.

30. Varshney, U., *Pervasive healthcare and wireless health monitoring.* Mobile Networks and Applications, 2007. **12**(2-3): p. 113-127.

31. Dias, N.S., et al., *Wireless instrumentation system based on dry electrodes for acquiring EEG signals.* Medical engineering & physics, 2012. **34**(7): p. 972-981.

32. Parthasarathy, J., et al. *Battery-operated high-bandwidth multi-channel wireless neural recording system using 802.11 b*. in *Engineering in Medicine and Biology Society, 2006. EMBS'06. 28th Annual International Conference of the IEEE*. 2006. IEEE.

33. Sneha, S. and U. Varshney, *A wireless ECG monitoring system for pervasive healthcare.* International Journal of Electronic Healthcare, 2007. **3**(1): p. 32-50.

34. Khoor, S., et al. *Telemedicine ECG-telemetry with Bluetooth technology*. in *Computers in Cardiology 2001*. 2001. IEEE.

35. Akahori, A., Y. Kishimoto, and K. Oguri. *Estimate activity for M-health using one three-axis accelerometer*. in *Medical Devices and Biosensors, 2006. 3rd IEEE/EMBS International Summer School on*. 2006. IEEE.

36. Scully, C.G., et al., *Physiological parameter monitoring from optical recordings with a mobile phone.* Biomedical Engineering, IEEE Transactions on, 2012. **59**(2): p. 303-306.

37. Asada, H.H., et al., *Mobile monitoring with wearable photoplethysmographic biosensors.* Engineering in Medicine and Biology Magazine, IEEE, 2003. **22**(3): p. 28-40.

38. Zhu, F., et al., *The use of mobile devices in aiding dietary assessment and evaluation.* Selected Topics in Signal Processing, IEEE Journal of, 2010. **4**(4): p. 756-766.

39. Grimes, A., V. Kantroo, and R.E. Grinter. *Let's play!: mobile health games for adults*. in *Proceedings of the 12th ACM international conference on Ubiquitous computing*. 2010. ACM.

40. Pollak, J., et al., *It's time to eat! Using mobile games to promote healthy eating.* Pervasive Computing, IEEE, 2010. **9**(3): p. 21-27.

41. Gammon, D., et al., *Parent-child interaction using a mobile and wireless system for blood glucose monitoring.* Journal of medical Internet research, 2005. **7**(5).

42. Cho, J.-H., et al., *Mobile communication using a mobile phone with a glucometer for glucose control in Type 2 patients with diabetes: as effective as an Internet-based glucose monitoring system.* Journal of Telemedicine and Telecare, 2009. **15**(2): p. 77-82.

43. Conkle, J.P., B.J. Camp, and B.E. Welch, *Trace Composition of Human Respiratory Gas.* Archives of Environmental Health, 1975. **30**(6): p. 290.

44. Barkley, J., et al., *Gas chromatography mass spectrometry computer analysis of volatile halogenated hydrocarbons in man and his environment—a multimedia environmental study.* Biological Mass Spectrometry, 1980. **7**(4): p. 139-147.

45. Krotoszynski, B., et al., *Characterization of human expired air: a promising investigative and diagnostic technique.* Journal of chromatographic science, 1977. **15**(7): p. 239-244.

46. Krotoszynski, B.K., G.M. Bruneau, and H.J. O'Neill, *Measurement of chemical inhalation exposure in urban population in the presence of endogenous effluents.* Journal of Analytical Toxicology, 1979. **3**(6): p. 225-234.

47. Risby, T.H. and S. Solga, *Current status of clinical breath analysis.* Applied Physics B: Lasers and Optics, 2006. **85**(2): p. 421-426.

48. Farhi, L., *Elimination of inert gas by the lung.* Respiration physiology, 1967. **3**(1): p. 1-11.

49. King, J., et al., *Isoprene and acetone concentration profiles during exercise on an ergometer.* Journal of Breath Research, 2009. **3**(2): p. 027006.

50. King, J., et al., *A mathematical model for breath gas analysis of volatile organic compounds with special emphasis on acetone.* Journal of mathematical biology, 2011. **63**(5): p. 959-999.

51. King, J., et al., *Dynamic profiles of volatile organic compounds in exhaled breath as determined by a coupled PTR-MS/GC-MS study.* Physiological measurement, 2010. **31**(9): p. 1169.

52. Fernandez, J., et al., *Trichloroethylene exposure. Simulation of uptake, excretion, and metabolism using a mathematical model.* British journal of industrial medicine, 1977. **34**(1): p. 43-55.

53. Andersen, M.E., *A physiologically based toxicokinetic description of the metabolism of inhaled gases and vapors: analysis at steady state.* Toxicology and applied pharmacology, 1981. **60**(3): p. 509-526.

54. Kim, K.H., S.A. Jahan, and E. Kabir, *A review of breath analysis for diagnosis of human health.* TrAC Trends in Analytical Chemistry, 2012.

55. Kalapos, M.P., *On the mammalian acetone metabolism: from chemistry to clinical implications.* Biochimica et Biophysica Acta (BBA)-General Subjects, 2003. **1621**(2): p. 122-139.

56. Smith, D. and P. Španěl, *Selected ion flow tube mass spectrometry (SIFT-MS) for on-line trace gas analysis.* Mass Spectrometry Reviews, 2004. **24**(5): p. 661-700.

57. Sulway, M. and J. Malins, *Acetone in diabetic ketoacidosis.* The Lancet, 1970. **296**(7676): p. 736-740.

58. Wang, C., A. Mbi, and M. Shepherd, *A study on breath acetone in diabetic patients using a cavity ringdown breath analyzer: Exploring correlations of breath acetone with blood glucose and glycohemoglobin a1c.* Sensors Journal, IEEE, 2010. **10**(1): p. 54-63.

59. Nelson, N., et al., *Exhaled isoprene and acetone in newborn infants and in children with diabetes mellitus.* Pediatric research, 1998. **44**(3): p. 363-367.

60. Kneepkens, F., G. Lepage, and C.C. Roy, *The potential of the hydrocarbon breath test as a measure of lipid peroxidation.* Free Radical Biology and Medicine, 1994. **17**(2): p. 127-160.

61. Hansen, T.K., et al., *Intensive insulin therapy exerts antiinflammatory effects in critically ill patients and counteracts the adverse effect of low mannose-binding lectin levels.* Journal of Clinical Endocrinology & Metabolism, 2003. **88**(3): p. 1082-1088.

62. Aghdassi, E., et al., *Antioxidant vitamin supplementation in Crohn's disease decreases oxidative stress: a randomized controlled trial.* The American journal of gastroenterology, 2003. **98**(2): p. 348-353.

63. Paredi, P., S.A. Kharitonov, and P.J. Barnes, *Elevation of exhaled ethane concentration in asthma.* American journal of respiratory and critical care medicine, 2000. **162**(4): p. 1450-1454.

64. Olopade, C.O., et al., *Exhaled pentane levels in acute asthma.* CHEST Journal, 1997. **111**(4): p. 862-865.

65. PAREDI, P., et al., *Exhaled ethane, a marker of lipid peroxidation, is elevated in chronic obstructive pulmonary disease.* American journal of respiratory and critical care medicine, 2000. **162**(2): p. 369-373.

66. Schubert, J., et al., *Application of a new method for analysis of exhaled gas in critically ill patients.* Intensive care medicine, 1998. **24**(5): p. 415-421.

67. Scholpp, J., et al., *Breath markers and soluble lipid peroxidation markers in critically ill patients.* Clinical chemistry and laboratory medicine, 2002. **40**(6): p. 587-594.

68. Scislowski, P.W.D. and K. Pickard, *The Regulation of Transaminative Flux of Methionine in Rat Liver Mitochondria.* Archives of Biochemistry and Biophysics, 1994. **314**(2): p. 412-416.

69. Chen, S., L. Zieve, and V. Mahadevan, *Mercaptans and dimethyl sulfide in the breath of patients with cirrhosis of the liver. Effect of feeding methionine.* The Journal of laboratory and clinical medicine, 1970. **75**(4): p. 628.

70. Tangerman, A., M. Meuwese-Arends, and J. van Tongeren, *New methods for the release of volatile sulfur compounds from human serum: its determination by Tenax trapping and gas chromatography and its application in liver diseases.* The Journal of laboratory and clinical medicine, 1985. **106**(2): p. 175.

71. Studer, S., et al., *Patterns and significance of exhaled-breath biomarkers in lung transplant recipients with acute allograft rejection.* The Journal of heart and lung transplantation: the official publication of the International Society for Heart Transplantation, 2001. **20**(11): p. 1158.

72. Moncada, S., R. Palmer, and E. Higgs, *Nitric oxide: physiology, pathophysiology, and pharmacology.* Pharmacological reviews, 1991. **43**(2): p. 109-142.

73. Palmer, R., A. Ferrige, and S. Moncada, *Nitric oxide release accounts for the biological activity of endothelium-derived relaxing factor.* 1987.

74. Nijkamp, F. and G. Folkerts, *Nitric oxide and bronchial hyperresponsiveness.* Archives internationales de pharmacodynamie et de therapie, 1995. **329**(1): p. 81.

75. Gaston, B., et al., *The biology of nitrogen oxides in the airways.* American journal of respiratory and critical care medicine, 1994. **149**(2): p. 538-551.

76. Pijnenburg, M. and J. De Jongste, *Exhaled nitric oxide in childhood asthma: a review.* Clinical & Experimental Allergy, 2008. **38**(2): p. 246-259.

77. Kharitonov, S., et al., *Increased nitric oxide in exhaled air of asthmatic patients.* The Lancet, 1994. **343**(8890): p. 133-135.

78. Alving, K., E. Weitzberg, and J. Lundberg, *Increased amount of nitric oxide in exhaled air of asthmatics.* European Respiratory Journal, 1993. **6**(9): p. 1368-1370.

79. Hamid, Q., et al., *Induction of nitric oxide synthase in asthma.* The Lancet, 1993. **342**(8886): p. 1510-1513.

80. Saleh, D., et al., *Increased formation of the potent oxidant peroxynitrite in the airways of asthmatic patients is associated with induction of nitric oxide synthase: effect of inhaled glucocorticoid.* The FASEB journal, 1998. **12**(11): p. 929-937.

81. Kharitonov, S.A., *Exhaled markers of inflammatory lung diseases: ready for routine monitoring?* Swiss Medical Weekly, 2004. **134**(13/14): p. 175-192.

82. Dupont, L.J., et al., *Exhaled nitric oxide correlates with airway hyperresponsiveness in steroid-naive patients with mild asthma.* American journal of respiratory and critical care medicine, 1998. **157**(3): p. 894-898.

83. Dupont, L.J., M.G. Demedts, and G.M. Verleden, *Prospective evaluation of the validity of exhaled nitric oxide for the diagnosis of asthma.* CHEST Journal, 2003. **123**(3): p. 751-756.

84. Lindberg, L., et al., *Breath alcohol concentration determined with a new analyzer using free exhalation predicts almost precisely the arterial blood alcohol concentration.* Forensic science international, 2007. **168**(2): p. 200-207.

85. McGill, C., G. Malik, and S.W. Turner, *Validation of a hand-held exhaled nitric oxide analyzer for use in children.* Pediatric pulmonology, 2006. **41**(11): p. 1053-1057.

86. Paul, J., et al., *Both the OxyArm™ and Capnoxygen mask provide clinically useful capnographic monitoring capability in volunteers.* Canadian Journal of Anaesthesia, 2003. **50**(2): p. 137-142.

87. Vreman, H., et al., *Evaluation of a fully automated end-tidal carbon monoxide instrument for breath analysis.* Clinical chemistry, 1996. **42**(1): p. 50-56.

88. Coulange, M., et al., *Reliability of new pulse CO-oximeter in victims of carbon monoxide poisoning.* 2008.

89. Elitsur, Y., et al., *Urea breath test in children: the United States prospective, multicenter study.* Helicobacter, 2009. **14**(2): p. 134-140.

90. Amann, A., P. Spanel, and D. Smith, *Breath analysis: the approach towards clinical applications.* Mini reviews in medicinal chemistry, 2007. **7**(2): p. 115-129.

91. Phillips, M., et al., *Heart allograft rejection: detection with breath alkanes in low levels (the HARDBALL study).* The Journal of heart and lung transplantation : the official publication of the International Society for Heart Transplantation, 2004. **23**(6): p. 701-708.

92. Sehnert, S.S., et al., *Breath biomarkers for detection of human liver diseases: preliminary study.* Biomarkers, 2002. **7**(2): p. 174-187.

93. Ghoos, Y., et al., *Porous-layer open-tubular gas chromatography in combination with an ion trap detector to assess volatile metabolites in human breath.* Biological Mass Spectrometry, 1989. **18**(8): p. 613-616.

94. Deng, C., X. Zhang, and N. Li, *Investigation of volatile biomarkers in lung cancer blood using solid-phase microextraction and capillary gas chromatography-mass*

spectrometry. Journal of chromatography. B, Analytical technologies in the biomedical and life sciences, 2004. **808**(2): p. 269.

95. Ligor, M., et al., *Determination of volatile organic compounds in exhaled breath of patients with lung cancer using solid phase microextraction and gas chromatography mass spectrometry.* Clinical chemistry and laboratory medicine, 2009. **47**(5): p. 550-560.

96. Buszewski, B., et al., *Analysis of exhaled breath from smokers, passive smokers and non-smokers by solid-phase microextraction gas chromatography/mass spectrometry.* Biomedical Chromatography, 2009. **23**(5): p. 551-556.

97. Adams, N. and D. Smith, *The selected ion flow tube (SIFT); a technique for studying ion-neutral reactions.* International Journal of Mass Spectrometry and Ion Physics, 1976. **21**(3): p. 349-359.

98. Smith, D., *The ion chemistry of interstellar clouds.* Chemical reviews, 1992. **92**(7): p. 1473-1485.

99. Delany, A., F. Melchior, and A. Wartburg, *Modification of a commerical NOx detector for high sensitivity.* Review of Scientific Instruments, 1982. **53**(12): p. 1899-1902.

100. Baldwin, S.R., et al., *Oxidant activity in expired breath of patients with adult respiratory distress syndrome.* The Lancet, 1986. **327**(8471): p. 11-14.

101. Robinson, J.K., M.J. Bollinger, and J.W. Birks, *Luminol/H2O2 chemiluminescence detector for the analysis of nitric oxide in exhaled breath.* Analytical chemistry, 1999. **71**(22): p. 5131-5136.

102. Roller, C., et al., *Simultaneous NO and CO_2 measurement in human breath with a single IV-VI mid-infrared laser.* Optics letters, 2002. **27**(2): p. 107-109.

103. Baum, M.M., et al., *Measurement of acetylene in breath by ultraviolet absorption spectroscopy: Potential for noninvasive cardiac output monitoring.* Review of Scientific Instruments, 2003. **74**(6): p. 3104-3110.

104. Rodríguez-Fernández, J., et al., *Simple detector for oral malodour based on spectrofluorimetric measurements of hydrogen sulphide in mouth air.* Analytica chimica acta, 1999. **398**(1): p. 23-31.

105. Wang, C., S.T. Scherrer, and D. Hossain, *Measurements of cavity ringdown spectroscopy of acetone in the ultraviolet and near-infrared spectral regions:*

potential for development of a breath analyzer. Applied spectroscopy, 2004. **58**(7): p. 784-791.

106. Elixhauser, A. and P. Owens, *Reasons for being admitted to the hospital through the emergency department, 2003*, in *Statistical Brief #2*Fubruary 2006, Agency for Healthcare Research and Quality: Rockville, Md.

107. Dragonieri, S., et al., *An electronic nose in the discrimination of patients with asthma and controls.* Journal of Allergy and Clinical Immunology, 2007. **120**(4): p. 856-862.

108. Gustafsson, L.E., et al., *Endogenous nitric oxide is present in the exhaled air of rabbits, guinea pigs and humans.* Biochemical and biophysical research communications, 1991. **181**(2): p. 852-857.

109. *World Health Organization Fact Sheet. Fact Sheet number 307*, 2011.

110. *Summary Health Statistics for U.S. Adults: National Health Interview Survey* 2011.

111. *Summary Health Statistics for U.S. Children: National Health Interview Survey.* 2011.

112. *National Asthma Education and Prevention Program. Expert Panel Report 3: Guidelines for the Diagnosis and Management of Asthma.* NIH Publication No. 07-4051, 2007.

113. Gratziou, C., et al., *Influence of atopy on exhaled nitric oxide in patients with stable asthma and rhinitis.* European Respiratory Journal, 1999. **14**(4): p. 897-901.

114. Baraldi, E., et al., *Corticosteroids decrease exhaled nitric oxide in children with acute asthma.* The Journal of pediatrics, 1997. **131**(3): p. 381-385.

115. Guo, F.H., et al., *Molecular mechanisms of increased nitric oxide (NO) in asthma: evidence for transcriptional and post-translational regulation of NO synthesis.* The Journal of Immunology, 2000. **164**(11): p. 5970-5980.

116. Redington, A., et al., *Increased expression of inducible nitric oxide synthase and cyclo-oxygenase-2 in the airway epithelium of asthmatic subjects and regulation by corticosteroid treatment.* Thorax, 2001. **56**(5): p. 351-357.

117. Warke, T., et al., *Exhaled nitric oxide correlates with airway eosinophils in childhood asthma.* Thorax, 2002. **57**(5): p. 383-387.

118. Berry, M., et al., *The use of exhaled nitric oxide concentration to identify eosinophilic airway inflammation: an observational study in adults with asthma.* Clinical & Experimental Allergy, 2005. **35**(9): p. 1175-1179.

119. Lim, S., et al., *Relationship between exhaled nitric oxide and mucosal eosinophilic inflammation in mild to moderately severe asthma.* Thorax, 2000. **55**(3): p. 184-188.

120. Smith, A.D., et al., *Diagnosing asthma comparisons between exhaled nitric oxide measurements and conventional tests.* American journal of respiratory and critical care medicine, 2004. **169**(4): p. 473-478.

121. Zietkowski, Z., et al., *Comparison of exhaled nitric oxide measurement with conventional tests in steroid-naive asthma patients.* Journal of Investigational Allergology and Clinical Immunology, 2006. **16**(4): p. 239.

122. Payne, D.N., et al., *Relationship between exhaled nitric oxide and mucosal eosinophilic inflammation in children with difficult asthma, after treatment with oral prednisolone.* American journal of respiratory and critical care medicine, 2001. **164**(8): p. 1376-1381.

123. Massaro, A.F., et al., *Expired nitric oxide levels during treatment of acute asthma.* American journal of respiratory and critical care medicine, 1995. **152**(2): p. 800-803.

124. Saito, J., et al., *Exhaled nitric oxide as a marker of airway inflammation for an epidemiologic study in schoolchildren.* Journal of allergy and clinical immunology, 2004. **114**(3): p. 512-516.

125. Saito, J., et al., *Off-line fractional exhaled nitric oxide measurement is useful to screen allergic airway inflammation in an adult population.* Journal of Asthma, 2007. **44**(10): p. 805-810.

126. Kharitonov, S.A., D.H. Yates, and P.J. Barnes, *Inhaled glucocorticoids decrease nitric oxide in exhaled air of asthmatic patients.* American journal of respiratory and critical care medicine, 1996. **153**(1): p. 454-457.

127. Smith, A.D., et al., *Use of exhaled nitric oxide measurements to guide treatment in chronic asthma.* New England Journal of Medicine, 2005. **352**(21): p. 2163-2173.

128. Sylvester, J. and S. Permutt, *Exhaled NO: first, hold your breath.* Journal of Applied Physiology, 2001. **91**(1): p. 474-476.

129. Phillips, C.R., G.D. Giraud, and W.E. Holden, *Exhaled nitric oxide during exercise: site of release and modulation by ventilation and blood flow.* Journal of Applied Physiology, 1996. **80**(6): p. 1865-1871.

130. Lefevere, L., et al., *Nasal nitric oxide.* Acta oto-rhino-laryngologica Belgica, 2000. **54**(3): p. 271.

131. Hyde, R.W., et al., *Determination of production of nitric oxide by lower airways of humans—theory.* Journal of Applied Physiology, 1997. **82**(4): p. 1290-1296.

132. Silkoff, P.E., *ATS/ERS Recommendations for Standardized Procedures for the Online and Offline Measurement of Exhaled Lower Respiratory Nitric Oxide and NasalNitric Oxide, 2005; American Thoracic Society Documents Nasal nitric oxide: longitudinal reproducibility and the effects of a nasal allergen challenge in patients with allergic rhinitis.* Chest, 2004. **126**: p. 1013-1014.

133. Silkoff, P., et al., *Recommendations for standardized procedures for the online and offline measurement of exhaled lower respiratory nitric oxide and nasal nitric oxide in adults and children—1999.* Am J Respir Crit Care Med, 1999. **160**(2104): p. 17.

134. Baraldi, E., et al., *Measurement of exhaled nitric oxide in children, 2001 E. Baraldi and JC de Jongste on behalf of the Task Force.* European Respiratory Journal, 2002. **20**(1): p. 223-237.

135. Kharitonov, S., K. Alving, and P. Barnes, *Exhaled and nasal nitric oxide measurements: recommendations. The European respiratory society task force.* European Respiratory Journal, 1997. **10**(7): p. 1683-1693.

136. Borrill, Z., et al., *A comparison of exhaled nitric oxide measurements performed using three different analysers.* Respiratory medicine, 2006. **100**(8): p. 1392-1396.

137. Müller, K., et al., *Comparison of exhaled nitric oxide analysers.* Respiratory medicine, 2005. **99**(5): p. 631-637.

138. Prabhakar, A., et al., *Ultrasensitive Detection of Nitrogen Oxides over a Nanoporous Membrane.* Analytical chemistry, 2010.

139. Wang, R., et al., *A Microfluidic-Colorimetric Sensor for Continuous Monitoring of Reactive Environmental Chemicals.* Sensors Journal, IEEE, 2012. **12**(5): p. 1529-1535.

140. Ochiai, N., et al., *Analysis of volatile sulphur compounds in breath by gas chromatography-mass spectrometry using a three-stage cryogenic trapping preconcentration system.* Journal of Chromatography B: Biomedical Sciences and Applications, 2001. **762**(1): p. 67-75.

141. Grote, C. and J. Pawliszyn, *Solid-phase microextraction for the analysis of human breath.* Analytical chemistry, 1997. **69**(4): p. 587-596.

142. Konvolina, G. and H. Haick, *The Effect of Humidity on Nanoparticle-Based Chemiresistors: A Comparison between Synthetic and Real-World Samples.* ACS Applied Materials & Interfaces, 2011.

143. Burns, W.F., et al., *Problems with a Nafion® membrane dryer for drying chromatographic samples.* Journal of Chromatography A, 1983. **269**(0): p. 1-9.

144. Foulger, B.E. and P.G. Simmonds, *Drier for field use in the determination of trace atmospheric gases.* Analytical chemistry, 1979. **51**(7): p. 1089-1090.

145. Leckrone, K.J. and J.M. Hayes, *Efficiency and Temperature Dependence of Water Removal by Membrane Dryers.* Analytical chemistry, 1997. **69**(5): p. 911-918.

146. Španěl, P. and D. Smith, *On-line measurement of the absolute humidity of air, breath and liquid headspace samples by selected ion flow tube mass spectrometry.* Rapid Communications in Mass Spectrometry, 2001. **15**(8): p. 563-569.

147. Boshier, P.R., et al., *On-line, real time monitoring of exhaled trace gases by SIFT-MS in the perioperative setting: a feasibility study.* Analyst, 2011. **136**(16): p. 3233-3237.

148. King, J., et al., *Physiological modeling of isoprene dynamics in exhaled breath.* Journal of theoretical biology, 2010. **267**(4): p. 626-637.

149. King, J., et al., *A modeling-based evaluation of isothermal rebreathing for breath gas analyses of highly soluble volatile organic compounds.* Journal of Breath Research, 2012. **6**: p. 016005.

150. Diskin, A.M., P. Španěl, and D. Smith, *Time variation of ammonia, acetone, isoprene and ethanol in breath: a quantitative SIFT-MS study over 30 days.* Physiological measurement, 2003. **24**: p. 107.

151. King, J., et al., *Measurement of endogenous acetone and isoprene in exhaled breath during sleep.* Physiological measurement, 2012. **33**: p. 413.

152. American Thoracic Society, E.R.S., *ATS/ERS recommendations for standardized procedures for the online and offline measurement of exhaled lower respiratory nitric oxide and nasal nitric oxide, 2005.* Am J Respir Crit Care Med, 2005. **171**: p. 912-930.

153. Prabhakar, A., et al., *Online sample conditioning for portable breath analyzers.* Analytical chemistry, 2012.

154. Childs, E. and N. Collis-George, *The permeability of porous materials.* Proceedings of the Royal Society of London. Series A. Mathematical and Physical Sciences, 1950. **201**(1066): p. 392-405.

155. Bear, J., *Dynamics of fluids in porous media*1988: Dover publications.

156. Tsilingiris, P., *Thermophysical and transport properties of humid air at temperature range between 0 and 100 C.* Energy Conversion and Management, 2008. **49**(5): p. 1098-1110.

157. Zhang, X. and L. Qiu, *Moisture transport and adsorption on silica gel-calcium chloride composite adsorbents.* Energy Conversion and Management, 2007. **48**(1): p. 320-326.

158. Glueckauf, E. and J. Coates, *241. Theory of chromatography. Part IV. The influence of incomplete equilibrium on the front boundary of chromatograms and on the effectiveness of separation.* J. Chem. Soc., 1947: p. 1315-1321.

159. Sircar, S. and J. Hufton, *Why does the linear driving force model for adsorption kinetics work?* Adsorption, 2000. **6**(2): p. 137-147.

160. Joly, A., V. Volpert, and A. Perrard. *Dynamic Adsorption with FEMLAB, Modeling breakthrough curves of gaseous pollutants through activated carbon beds*. 2005.

161. Park, I. and K.S. Knaebel, *ADSORPTION BREAKTHROUGH BEHAVIOR - UNUSUAL EFFECTS AND POSSIBLE CAUSES.* Aiche Journal, 1992. **38**(5): p. 660-670.

162. Kamiuto, K., Ermalina, and K. Ihara, *CO2 adsorption equilibria of the honeycomb zeolite beds.* Applied Energy, 2001. **69**(4): p. 285-292.

163. Mămăligă, I., C. Baciu, and S. Petrescu, *STUDY OF ADSORPTION EQUILIBRIUM OF SOME WET AIR-COMPOSITE MATERIAL SYSTEMS.* Environmental Engineering & Management Journal (EEMJ), 2009. **8**(2): p. 253-257.

164. Ellerbee, A.K., et al., *Quantifying colorimetric assays in paper-based microfluidic devices by measuring the transmission of light through paper.* Analytical chemistry, 2009. **81**(20): p. 8447-8452.

165. Popov, A.I. and W.W. Wendlandt, *The Methylamine Complexes of the Rare Earth (III) Chlorides1*. Journal of the American Chemical Society, 1955. **77**(4): p. 857-859.

166. Hay, R. and M. Bond, *Kinetics of the decarboxylation of acetoacetic acid.* Australian Journal of Chemistry, 1967. **20**(9): p. 1823-1828.

167. McGarry, J. and D. Foster, *Regulation of hepatic fatty acid oxidation and ketone body production.* Annual review of biochemistry, 1980. **49**(1): p. 395-420.

168. Garber, A., et al., *Hepatic ketogenesis and gluconeogenesis in humans.* Journal of Clinical Investigation, 1974. **54**(4): p. 981.

169. Reichard Jr, G., et al., *Ketone-body production and oxidation in fasting obese humans.* Journal of Clinical Investigation, 1974. **53**(2): p. 508.

170. Serra, D., et al., *Regulation of mitochondrial 3-hydroxy-3-methylglutaryl-coenzyme A synthase protein by starvation, fat feeding, and diabetes.* Archives of biochemistry and biophysics, 1993. **307**(1): p. 40-45.

171. Randle, P., E. Newsholme, and P. Garland, *Regulation of glucose uptake by muscle. 8. Effects of fatty acids, ketone bodies and pyruvate, and of alloxan-diabetes and starvation, on the uptake and metabolic fate of glucose in rat heart and diaphragm muscles.* Biochemical Journal, 1964. **93**(3): p. 652.

172. Finn, P.F. and J.F. Dice, *Proteolytic and lipolytic responses to starvation.* Nutrition, 2006. **22**(7): p. 830-844.

173. Nair, K.S., et al., *Effect of beta-hydroxybutyrate on whole-body leucine kinetics and fractional mixed skeletal muscle protein synthesis in humans.* Journal of Clinical Investigation, 1988. **82**(1): p. 198.

174. Pardridge, W.M., *Blood-brain barrier transport of glucose, free fatty acids, and ketone bodies*, in *Fuel Homeostasis and the Nervous System*1991, Springer. p. 43-53.

175. Hasselbalch, S.G., et al., *Blood-brain barrier permeability of glucose and ketone bodies during short-term starvation in humans.* American Journal of Physiology-Endocrinology And Metabolism, 1995. **268**(6): p. E1161-E1166.

176. Hawkins, R.A., A.M. Mans, and D.W. Davis, *Regional ketone body utilization by rat brain in starvation and diabetes.* American Journal of Physiology-Endocrinology And Metabolism, 1986. **250**(2): p. E169-E178.

177. Laffel, L., *Ketone bodies: a review of physiology, pathophysiology and application of monitoring to diabetes.* Diabetes/metabolism research and reviews, 1999. **15**(6): p. 412-426.

178. Bonnefont, J., et al., *The fasting test in paediatrics: application to the diagnosis of pathological hypo-and hyperketotic states.* European journal of pediatrics, 1990. **150**(2): p. 80-85.

179. Atkins, R.D., *Dr. Atkins' new diet revolution*2002: M. Evans.

180. Paoli, A., L. Cenci, and K.A. Grimaldi, *Effect of Ketogenic Mediterranean diet with phytoextracts and low carbohydrates/high-protein meals on weight, cardiovascular risk factors, body composition and diet compliance in Italian council employees.* Nutr J, 2011. **10**: p. 112.

181. Freeman, J.M., E.H. Kossoff, and A.L. Hartman, *The ketogenic diet: one decade later.* Pediatrics, 2007. **119**(3): p. 535-543.

182. Kossoff, E.H., et al., *Optimal clinical management of children receiving the ketogenic diet: recommendations of the International Ketogenic Diet Study Group.* Epilepsia, 2009. **50**(2): p. 304-317.

183. Sasaki, H., et al., *Response of Acetone in Expired Air During Graded and Prolonged Exercise.* Advances in exercise and sports physiology, 2011. **16**(3): p. 97-100.

184. Koeslag, J., T. Noakes, and A. Sloan, *Post-exercise ketosis.* The Journal of physiology, 1980. **301**(1): p. 79-90.

185. Newton, C.A. and P. Raskin, *Diabetic ketoacidosis in type 1 and type 2 diabetes mellitus: clinical and biochemical differences.* Archives of internal medicine, 2004. **164**(17): p. 1925.

186. Balasubramanyam, A., et al., *New profiles of diabetic ketoacidosis: type 1 vs type 2 diabetes and the effect of ethnicity.* Archives of internal medicine, 1999. **159**(19): p. 2317.

187. Miles, J., et al., *Effects of free fatty acid availability, glucagon excess, and insulin deficiency on ketone body production in postabsorptive man.* Journal of Clinical Investigation, 1983. **71**(6): p. 1554.

188. Kitabchi, A.E., et al., *Management of hyperglycemic crises in patients with diabetes.* Diabetes care, 2001. **24**(1): p. 131-153.

189. Engelgau, M.M., et al., *The evolving diabetes burden in the United States.* Annals of Internal Medicine, 2004. **140**(11): p. 945-950.

190. Maldonado, M.R., et al., *Economic Impact of Diabetic Ketoacidosis in a Multiethnic Indigent Population Analysis of costs based on the precipitating cause.* Diabetes care, 2003. **26**(4): p. 1265-1269.

191. Auchterlonie, A. and O.E. Okosieme, *Preventing diabetic ketoacidosis: do patients adhere to sick-day rules?* Clinical Medicine, 2013. **13**(1): p. 120-120.

192. Kim, S., *Burden of Hospitalizations Primarily Due to Uncontrolled Diabetes Implications of inadequate primary health care in the United States.* Diabetes care, 2007. **30**(5): p. 1281-1282.

193. The Royal Children's Hospital. *Ketogenic Diet*. [cited 2013 April 21]; Available from: http://www.rch.org.au/cep/treatments/Ketogenic_Diet/#What_is_required_at_home.

194. Wallace, T. and D. Matthews, *Recent advances in the monitoring and management of diabetic ketoacidosis.* Qjm, 2004. **97**(12): p. 773-780.

195. Lorenz, R.A., et al., *Tests of glycemia in diabetes.* Diabetes care, 2003. **26**: p. 1.

196. Federici, M.O. and M.M. Benedetti, *Ketone bodies monitoring.* Diabetes Research and Clinical Practice, 2006. **74**: p. S77-S81.

197. Byrne, H., et al., *Evaluation of an electrochemical sensor for measuring blood ketones.* Diabetes care, 2000. **23**(4): p. 500-503.

198. Ham, M.R., P. Okada, and P.C. White, *Bedside ketone determination in diabetic children with hyperglycemia and ketosis in the acute care setting.* Pediatric diabetes, 2004. **5**(1): p. 39-43.

199. Musa-Veloso, K., S.S. Likhodii, and S.C. Cunnane, *Breath acetone is a reliable indicator of ketosis in adults consuming ketogenic meals.* The American journal of clinical nutrition, 2002. **76**(1): p. 65-70.

200. Musa-Veloso, K., et al., *Epilepsy and the ketogenic diet: assessment of ketosis in children using breath acetone.* Pediatr Res, 2002. **52**(3): p. 443-8.

201. Deng, C., et al., *Determination of acetone in human breath by gas chromatography-mass spectrometry and solid-phase microextraction with on-fiber derivatization.* Journal of chromatography. B, 2004. **810**(2): p. 269-275.

202. Guo, D., et al., *Diabetes identification and classification by means of a breath analysis system*, in *Medical Biometrics*2010, Springer. p. 52-63.

203. Turner, C., et al., *Breath acetone concentration decreases with blood glucose concentration in type I diabetes mellitus patients during hypoglycaemic clamps.* Journal of breath research, 2009. **3**(4): p. 046004.

204. Hartman, A.L. and E.P. Vining, *Clinical aspects of the ketogenic diet.* Epilepsia, 2007. **48**(1): p. 31-42.